Calhoun: The NPS Institutional Archive

DSpace Repository

Theses and Dissertations | 1. Thesis and Dissertation Collection, all items

2002-06

Microelectromechanical propulsion systems for spacecraft

Lemay, Scott A.

Monterey, California. Naval Postgraduate School

http://hdl.handle.net/10945/5883

This publication is a work of the U.S. Government as defined in Title 17, United States Code, Section 101. Copyright protection is not available for this work in the United States.

Downloaded from NPS Archive: Calhoun

http://www.nps.edu/library

Calhoun is the Naval Postgraduate School's public access digital repository for research materials and institutional publications created by the NPS community. Calhoun is named for Professor of Mathematics Guy K. Calhoun, NPS's first appointed -- and published -- scholarly author.

Dudley Knox Library / Naval Postgraduate School
411 Dyer Road / 1 University Circle
Monterey, California USA 93943

NAVAL POSTGRADUATE SCHOOL
Monterey, California

THESIS

MICROELECTROMECHANICAL PROPULSION SYSTEMS FOR SPACECRAFT

by

Scott A. Lemay

June 2002

Thesis Advisor:	Oscar Biblarz
Second Reader:	Jose Sinibaldi

Approved for public release; distribution is unlimited

THIS PAGE INTENTIONALLY LEFT BLANK

REPORT DOCUMENTATION PAGE			Form Approved OMB No. 0704-0188
Public reporting burden for this collection of information is estimated to average 1 hour per response, including the time for reviewing instruction, searching existing data sources, gathering and maintaining the data needed, and completing and reviewing the collection of information. Send comments regarding this burden estimate or any other aspect of this collection of information, including suggestions for reducing this burden, to Washington headquarters Services, Directorate for Information Operations and Reports, 1215 Jefferson Davis Highway, Suite 1204, Arlington, VA 22202-4302, and to the Office of Management and Budget, Paperwork Reduction Project (0704-0188) Washington DC 20503.			
1. AGENCY USE ONLY *(Leave blank)*	**2. REPORT DATE** June 2002	**3. REPORT TYPE AND DATES COVERED** Master's Thesis	
4. TITLE AND SUBTITLE: Microelectromechanical Propuslion Systems for Spacecraft			**5. FUNDING NUMBERS**
6. AUTHOR(S) Scott A. Lemay			
7. PERFORMING ORGANIZATION NAME(S) AND ADDRESS(ES) Naval Postgraduate School Monterey, CA 93943-5000			**8. PERFORMING ORGANIZATION REPORT NUMBER**
9. SPONSORING /MONITORING AGENCY NAME(S) AND ADDRESS(ES) N/A			**10. SPONSORING/MONITORING AGENCY REPORT NUMBER**
11. SUPPLEMENTARY NOTES The views expressed in this thesis are those of the author and do not reflect the official policy or position of the Department of Defense or the U.S. Government.			
12a. DISTRIBUTION / AVAILABILITY STATEMENT Distribution Statement (mix case letters)			**12b. DISTRIBUTION CODE**

13. ABSTRACT ***(maximum 200 words)***

This is a survey of current research on micropropulsion options for very small satellites (less than ten kilogram). The concentration of research and performance evaluations utilize Micro Systems Technology (MST) and Micro Electromechanical Systems technology (MEMS) integrated with existing theories. State of the art methods used for the design and manufacturing of MEMS devices are included to provide a size perspective of microthruster technology. Nine viable microthruster options are presented, including a detailed performance analysis of the Pulsed Plasma Thruster. Exploration of the future role of micropropulsion in space is the influential factor benefiting research efforts on extremely small scale microthrusters. Significant background information on astrodynamics is included to assist the intended reader: a student of Engineering Science with interest in the Aerospace Propulsion Industry.

14. SUBJECT TERMS Micro-Elecromechanical Systems, MEMS, Microelectromechanical Systems, Micro Systems Technology, MST, Propulsion, Thruster, Microthruster, Pulsed Plasma Thruster, PPT.			**15. NUMBER OF PAGES** 87
			16. PRICE CODE
17. SECURITY CLASSIFICATION OF REPORT Unclassified	**18. SECURITY CLASSIFICATION OF THIS PAGE** Unclassified	**19. SECURITY CLASSIFICATION OF ABSTRACT** Unclassified	**20. LIMITATION OF ABSTRACT** UL

NSN 7540-01-280-5500 Standard Form 298 (Rev. 2-89)
Prescribed by ANSI Std. 239-18

THIS PAGE INTENTIONALLY LEFT BLANK

Approved for public release; distribution is unlimited

MICROELECTROMECHANICAL PROPULSION SYSTEMS FOR SPACECRAFT

Scott A. Lemay
Lieutenant, United States Navy
B.S., University of South Carolina, 1995

Submitted in partial fulfillment of the
requirements for the degree of

MASTER OF SCIENCE IN ASTRONAUTICAL ENGINEERING

from the

NAVAL POSTGRADUATE SCHOOL
June 2002

Author: _____
Scott A. Lemay

Approved by: _____
Oscar Biblarz, Thesis Advisor

_____
Jose Sinibaldi, Second Reader

_____
Max F. Platzer, Chairman
Department of Aeronautics and Astronautics

THIS PAGE INTENTIONALLY LEFT BLANK

ABSTRACT

This is a survey of current research on micropropulsion options for very small satellites (less than ten kilogram). The concentration of research and performance evaluations utilize Micro Systems Technology (MST) and Micro Electromechanical Systems technology (MEMS) integrated with existing theories. State of the art methods used for the design and manufacturing of MEMS devices are included to provide a size perspective of microthruster technology. Nine viable microthruster options are presented, including a detailed performance analysis of the Pulsed Plasma Thruster. Exploration of the future role of micropropulsion in space is the influential factor benefiting research efforts on extremely small scale microthrusters. Significant background information on astrodynamics is included to assist the intended reader: a student of Engineering Science with interest in the Aerospace Propulsion Industry.

THIS PAGE INTENTIONALLY LEFT BLANK

TABLE OF CONTENTS

I. INTRODUCTION 1
A. BACKGROUND 1
B. MOTIVATION 2
1. MEMS Components 3
2. Application-Specific Integrated Microinstruments - ASIMS 3
C. SCOPE 4

II. MICROSYSTEM TECHNOLOGY 5
A. HISTORICAL BACKGROUND 5
B. MEMS 6
C. MICROENGINEERING 7
1. Lithography 8
2. Etching 9
3. Bulk Micromachining 10
4. Surface Micromachining 11
5. Excimer Laser Fabrication 12
6. LIGA (Lithography, Electroplating, and Molding) 13

III. ASTRONAUTICAL APPLICATIONS 15
A. ASTRODYNAMIC BACKGROUND 15
1. Notation 15
2. Orbital Drift 17
3. Orbit Definitions 17
B. ORBITAL MAINTENANCE 18
1. Orbit Changes 19
2. Station Keeping 19
3. Attitude Determination and Control 20
C. THRUST GENERATION 21

IV. MICROTHRUSTER TECHNOLOGY 23
A. PROPULSION OVERVIEW 23
B. COLD GAS MICROTHRUSTER 24
1. Effects on Scaling 25
C. FLIGHT AVAILABLE THRUSTERS 30
1. Solid Digital Thruster Design 30
2. Plasma Thrusters 32
3. Cold-Gas Thruster 32
D. EXPERIMENTAL THRUSTER OPTIONS 32
1. Resistojet 33
2. Colloidal Ion Thrusters -- Field Emission Array (FEA) 36
3. Resistojet -- Vaporizing liquid microthruster (VLM) 37
4. Resistojet -- Free Molecule Micro-Resistojet (FMMR) 38

5. Laser Ablation micro-Thruster (LAmT) 39
6. Vacuum Arc Thruster (VAT) 40

V. PULSED PLASMA THRUSTER (PPT) 41
A. HISTORY 41
B. MODELING/OPERATIONAL THEORY 43
C. DISADVANTAGES 50
D. USAGE 51

VI. SPACE MISSIONS 53
A. MISSION PLANNING 53
B. SCHEDULED MISSIONS 54
1. Vanguard I (Launched March 17, 1958) 55
2. OPAL (Launched January 26, 2000) 55
3. Snap-1 (Launched June 28, 2000) 57
4. University Nanosatellite Program 58
a. *Nanosat-1 (Expected Launch date: April 2003)* *59*
b. *Nanosat-2 (Expected Launch date: June 2003)* *59*
5. TechSat 21 63

VII. CONCLUSION 65
A. PRESENT WORK 65
B. CANDIDATES 65

LIST OF REFERENCES 67

INITIAL DISTRIBUTION LIST 71

LIST OF FIGURES

Figure 2-1. MEMS Market Forecast [From 3] 7
Figure 2-2. Simple MEMS Bulk Manufactured Beam [From 2]....10
Figure 2-3. Schematic of a Simple Surface Micromachined Cantilever Beam [From 2]...12
Figure 2-4. LIGA Micromachining Techniques. [From 2]....13
Figure 3-1. Two Dimensional Elementary Orbit [From 4]....16
Figure 3-2. Three-Dimensional orbit diagram with Celestial Coordinates [From 4] 16
Figure 3-3. Satellite orbits with i, j, k reference frame [After 4]....18
Figure 3-4. Thruster Arrangement for Attitude Control [From 6]....20
Figure 3-5. The DeLaval Nozzle [From 7]. 22
Figure 4-1. Boundary Layer Formation. [After 9]....27
Figure 4-2. Mach contours of laminar flow in an optimized MEMS thruster. [From 10]..28
Figure 4-3. Unit-less size comparison between flat and round nozzles of equal cross sectional areas. [From 9]....29
Figure 4-4. An Assembled MEMS Digital Thruster Array of 15 elements. [From 12] 31
Figure 4-5. Current Digital Propulsion Configuration. [From 12] 32
Figure 4-6. Image of Laboratory Resistojet design. [After 13] 34
Figure 4-7. Conceptual Diagram of an FEA. [From 11] 37
Figure 4-8. VLM DIAGRAM. [From 14] 38
Figure 4-9. FMMR, a) side view b) orthogonal view. [From 11] 39
Figure 5-1. Breech Fed Rectangular Geometry PPT. [After 16]....42
Figure 5-2. Breech Fed Coaxial Geometry PPT. [From 16]....43
Figure 5-3. Optimizing Teflon Fuel design. [From 16] 47
Figure 5-4. Current arc of Rectangular PPT Geometry. [From 16]....48
Figure 5-5. Current arc of Coaxial PPT with diode. [After 16]....48
Figure 5-6. Schematic of PPT-4, notice quenching diode. [From 16]....49
Figure 5-7. Breakdown of the Energy Processes and Efficiencies within the PPT. [From 17] 50
Figure 5-8. Air Force Research Lab's μPPT. [From 18] 52
Figure 6-1. Overview of application regions for different electrical microthruster options. 53
Figure 6-2. Mission Comparison of Propulsion System Masses modified from reference. [After 20] 54
Figure 6-3. Vanguard I on Test Stand 1956. [From 22] 55
Figure 6-4. OPAL in pre-launch testing. [From 23]....56
Figure 6-5. Aerospace Corporation’s Daughter Satellites (left) and Santa Clara’s Artemis Satellite (right).[From 23 and 24]....56
Figure 6-6. SNAP-1 propulsion subsystem. [From 25]....58
Figure 6-7. Possible Launch Configuration for Three Corner Sat and ION-F. [After 28] 60
Figure 6-8. Free Molecular Micro-Resistojet heater strip developed by Arizona State University for each 3CS. [From 28]....61
Figure 6-9. ION- F Micro Pulsed Plasma Thrusters. [From 29] 62
Figure 6-10. TechSat 21 Mission Concept. [From 19]....63

THIS PAGE INTENTIONALLY LEFT BLANK

LIST OF TABLES

Table 4-1. Micropropulsion Systems with Technology Issues. Estimated dry mass will vary to accommodate propellant requirements. Data obtained from references 2, 6, 9, 10, 11and 24. 23

THIS PAGE INTENTIONALLY LEFT BLANK

ACKNOWLEDGMENTS

"For I the Lord thy God will hold thy right hand, saying unto thee, Fear not; I will help thee."
Isaiah 41:13

I would like to thank Professor Oscar Biblarz for his patience, insight, and timely assistance. I would also like to thank Assistant Research Professor Doctor Jose Sinibaldi for his support, assistance, and conversations over the roar of a pulse detonation rocket engine. I am forever grateful for all their help.

Any endeavor would not be possible without support, and thus, I say thank you to my family: My wife Laura, my parents Raymond and Janet. Their assistance and encouragement was beyond measure.

Lastly, I say thank you those who were able help tame the "Dragon." Thank you for the humor, and of course, the thesis processing help.

THIS PAGE INTENTIONALLY LEFT BLANK

I. INTRODUCTION

A. BACKGROUND

Microsystems technology (MST) is poised, with proper research and development, to bring about the next technological breakthrough in the United States. Microelectromechanical systems (MEMS) research encompasses the miniaturization of systems containing electronic and mechanical components. Applications for this emerging technology have developed rapidly over the past few decades in sensor systems. In recent years, however, researchers have demonstrated additional applications in microvalve and microthruster technological improvements. Integration of MEMS into propulsion systems enables space flight demonstrations, which highlight their potential in aerospace system technology. MEMS allow engineers to generate revolutionary satellite designs by combining technological advances in sensors, actuators, information processing and storage, and thrusters through the miniaturization of these component systems. Small satellite technology has, therefore, begun to shift the design perspective away from large multi-use and long-lived spacecraft towards satellites that are small, single-function units with short mission duration. [1]

The main objective of most space agencies is to meet mission requirements with the lowest cost without compromising safety. In order to reduce spacecraft lifecycle costs and lead-time, without reducing performance, a different approach to spacecraft construction and design is needed. Miniaturization of components and systems is one area in which innovative concepts may yield very promising results. The launch vehicle, with orbit insertion, is one of the highest cost factors for space-based systems. These costs are directly related to spacecraft mass. Traditionally, the propulsion subsystem comprises 10% of the satellite platform mass, which has a direct correlation to the payload mass, power and volume requirements. Any reduction in mass, power or volume requirements is, therefore, desirable and would have a significant impact on mission cost. MEMS technology is the best method for obtaining very significant mass reductions. MEMS also allow for a new approach to space systems mission design through decentralization of control and operations. MEMS devices become an enabling technology through which a number of dispersed components, or even satellites, replace a

larger centralized unit, achieving greater efficiency and redundancy. All of which affects the bottom line - cost reduction. The cost savings are not only at the platform level, but also in the launchers, ground facilities, achieved by batch production, and the replacement of high-performance units with multiple standard performance parts. Because cost increases exponentially with performance, cost savings require a new way of thinking about the services demanded and the systems needed to provide those services. [1]

B. MOTIVATION

The history of the propulsion arm of the space industry is one of developing stronger and more durable systems. As the spacecraft size is reduced, the need for large thrust devices is eliminated and the propulsion subsystem is reduced in size and capability. MEMS are being developed that will reduce the size, weight, and thrust levels for a correspondingly smaller satellite. The space industry should closely follow research developments in search of system and components that are adaptable and able to be integrated with available elements. MEMS space applications will reduce the spacecraft size and mass. In order to utilize MEMS fully, new ways of addressing mission requirements are essential. Since ideal solutions are rare, the space industry will need to devote resources to new MEMS deployment issues. The two most critical limitations are the costs of development and a high susceptibility to radiation – a problem with all semiconductor materials.

The integration of MEMS into conventional space systems has occurred routinely through efforts to find sub-systems that are lighter, faster, and less expensive. MEMS devices are an enabling technology for the very small satellites. The early MEMS in space must be able to demonstrate optimal performance capabilities and meet the strict reliability requirements of the aerospace industry. To meet this goal, components need to comply with the conventional standards and the results compared. As with all unconventional components, different interfaces need to be addressed. The dimensions of standard mechanical connectors are similar to those of MEMS but the electrical power requirements are typically 3 V versus the more standard 28 V. In some cases, adding MEMS integration devices require an acceptable interface, which may result in a subsystem box similar in size to the conventional one it is supposed to replace. One

integration method that is being studied by the Air Force Research Laboratory (AFRL) uses a piggyback method to demonstrate flight performance. The AFRL research satellite, TECHSAT 21, will incorporate two microthrusters into the propulsion system, one as a redundant thruster. Such innovation serves as a flight qualification method by operating in parallel for observation and comparison purposes, thus, offering an additional redundancy with a low impact on the spacecraft budgets of mass, volume, and power. [1]

MEMS utilization will likely occur in one of two manners:

1. MEMS Components

The use of MEMS components integrated into the overall system which allows for thrust devices that are robust yet small enough to be incorporated into the small satellite design. The component aspect of MEMS can be utilized through the use of MEMS sensors incorporated into larger systems – for example, propellant tank leak detection. The industrial requirements will consist of adapting mission requirements to space available MEMS and of producing new MEMS at limited levels of development.

The introduction of MEMS propulsion systems in space vehicles is limited by the size of the spacecraft. A 1 kg satellite could use a microthruster for orbit changes whereas in a 10 kg satellite, the same microthruster would be limited to station keeping or attitude control

2. Application-Specific Integrated Microinstruments - ASIMS

As quality control improves, the next step might be to incorporate an entire propulsion system into one device. Application-specific integrated microinstrument (ASIM) creates various types of ultra-small satellite subsystems, which are custom designed for each satellite. Eventually complete nanosatellites about the size of a cigarette lighter or larger ones (the size of a soda bottle) will be available. Ideal candidates for subsystems design are sensor instrumentation, full payloads, on-board data handling, attitude determination and control, and propulsion. The propulsion subsystem could be easily integrated with few external parts and an improved manufacturing process. [2].

C. SCOPE

The scope of this thesis will focus on the currently available microthrusters and the exploration of the usefulness of the emerging MEMS propulsion systems. The question will be posed: Can MEMS components replace conventional components? Specifically:

1. Will MEMS eventually replace an entire propulsion subsystem, including propellant and flow control, into one integrated device and still meet performance requirements?

2. How small can a small thruster be? Currently the operational micro-, nano-, and pico- sized satellites use MEMS components in the attitude control, propulsion, and payload subsystems.

3. What opportunities for the application of these thrusters are identified? Although the efficiency and reliability performance available from a MEMS thruster systems is significantly lower than that achieved by existing macroscopic devices, the low cost, small size and low power requirements of the MEMS devices creates many application specific uses. In particular, we show that as spacecraft size and mass are reduced, the need for "large" thrust devices is removed. MEMS technologies may provide micro- and nano- thrusters to meet the requirements of lower mass and volume.

II. MICROSYSTEM TECHNOLOGY

A. HISTORICAL BACKGROUND

MEMS and Integrated Circuits (ICs) have the same origin, a laboratory accident. The age of miniaturization began on November 17, 1947 when Walter Brattain was studying how electrons behaved on the surface of a semiconductor and why these electrons interfered in building an amplifier. During the experiment, Brattain was unable to remove condensation that kept forming on the silicon. Out of frustration over this reoccurring problem, Brattain decided to dump the whole experiment under water. The device, now wet, created the largest amplification he had ever observed and solved his greatest problem in building an amplifier. When his fellow engineer, John Bardeen, saw what happened he suggested pushing a metal point into the silicon surrounded by distilled water. Another Bell-Lab engineer, William Shockley, provided the theoretical insight to deduce the reasoning behind Brattain's and Bardeen's laboratory results. With his insight, Shockley conceptualized the idea of the junction transistor: three layers of semiconductors piled together. The outermost pieces would be semiconductors with too many electrons, while the layer in the middle would have too few electrons. All this work led to a Nobel Prize for Brattain, Bardeen, and Shockley. [1]

Ten years after Brattain's discovery the scientific community treated the concept of miniaturization in different ways. Scientists like Isaac Asimov and Richard Feyman envisioned complete microsystems within a single silicon wafer while other scientists predicted that no transistor on a chip would ever be smaller than 10 μm. Modern computers utilize chips that are 100 times smaller than a micrometer. Ultra-large-scale-integration (ULSI) enables the fabrication of more than 10 million transistors and capacitors on a typical chip. ULSI-based microprocessors and microcomputers have revolutionized communication, entertainment, health care, manufacturing, management, and many other aspects of life. Large, expensive, and complex systems have been replaced by small, high performance, inexpensive integrated circuits. This growth in the functionality of microelectronic circuits has been limited by the processing power of the

chip. [1] The future of miniaturization has continued to be a favored topic of discussion. Dr. Feyman gave a famous presentation in 1959 at the American Physical Society titled *There's Plenty of Room at the Bottom*. It is during this speech he added some humor concerning the future of miniaturized IC devices, "What would be the utility of such machines? Who knows? Of course, a small automobile would only be useful for the mites to drive around in."

B. MEMS

Microelectromechanical systems (MEMS) is the next logical step in the silicon revolution which is transforming the conventional field of solid-state transducers. Where ICs are the integrated electrical and electronic systems onto a small package, MEMS are the integrated mechanical and electrical systems. The principal difference is that there are no moving parts to an electronic device, it is purely transistor based applications. Today MEMS make up one of the fastest growing markets. MEMS is a relatively new technology which exploits the existing microelectronics infrastructure to create complex mechanical devices of micron size. MEMS bring the incorporation of new types of functionality onto the chip, which will enable these chips to not only think, but to sense, act and communicate, as well. Extensive applications for these devices exist in both commercial and defense systems. MEMS are completely application driven and technology limited, and have, therefore, emerged as an interdisciplinary field that involves many areas of science and engineering. MEMS devices have proliferated into the commercial sector and are penetrating new markets in addition to the automotive, medical, and aerospace and defense markets which they continue to serve. As they now penetrate the communications (RF and optical), biomedical, consumer, and industrial markets. The future business projections of MEMS technology can be seen below in Figure 2-1. NEXUS is a European market forecasting company with a proven history of reliability and accuracy.

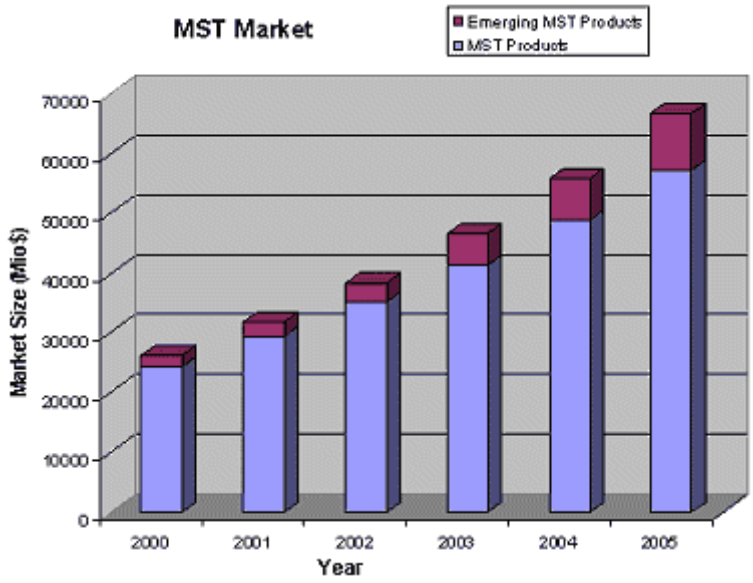

Figure 2-1. MEMS Market Forecast [From 3]

The aerospace industry has incorporated MEMS technology into a wide variety of system applications. The ability to integrate multiple components into a small package has reduced sensors, control and actuation systems, and propulsion subsystems in size and weight. NASA's recent budgetary constraints have resulted in the need to use progressive technologies, like MEMS, in order to achieve its goal of smaller, faster, less expensive and more capable spacecraft. MEMS are currently being used for many subsystems on a spacecraft such as the attitude control system with inertial reference sensors, actuators, fluid flow controllers, health monitoring systems, and propulsion systems.

C. MICROENGINEERING

Microengineering encompasses the technology and methods used to make three-dimensional structures that can only be viewed with an electron microscope. Microengineering is essential in MEMS construction. MEMS microstructures are manufactured in batch methods similar to IC chips used in the computer microchips. These photolithographic techniques can also be used to mass produce mechanical sensors and actuators physically integrated with electronic circuitry. In a production method similar to ICs, MEMS are developed from thin film materials. The same photolithographic techniques and batch fabrication methods used for ICs are also used for

MEMS. The four constructional technologies include: surface micromachining, bulk micromachining, excimer-laser micromachining, and "lithographie, galvanoformung, and abformung" (LIGA). LIGA is a German technology which translates to lithography, electroplating and molding. Microengineering has the capability to produce completely integrated systems (microsystems) by integrating microelectronic circuitry into micromachined structures. Although all MEMS fabrication techniques require a multi-step process, the ability to simultaneously manufacture large numbers of devices on a single silicon wafer reduces the overall cost per unit. Computer Aided Design (CAD) tools optimize the design and production process and the ability to proceed quickly from a prototype to high volume manufacturing are additional reasons to pursue MEMS technology. [2]

Each manufacturing process is based on the deposition of thin films of metal or crystalline material on a substrate, the application of patterned masks by photolithographic imaging, and the etching of the films to the mask. The sacrificial layer is a disposable material which keeps each substrate layer separated as the three-dimensional structure is being built. Extreme cleanliness and precision are required to ensure each substrate layer is correctly patterned during the deposition process. Two application methods are utilized to deposit the thin film materials; chemical reactions and physical reactions. Chemical vapor deposition, electrodeposition, epitaxy, and thermal oxidation create solid materials directly from chemical reactions in gas. They also create solid materials from liquid composition reactions with the substrate material. Physical vapor deposition, known as casting, moves the desired material directly onto the substrate. Casting has the advantage of achieving a smooth surface without exposure to product contamination. [2]

1. Lithography

The most decisive characteristic of a "MEMS device" is the use of lithography in its fabrication. Lithography is the technique used to transfer copies of a master pattern onto the surface of a solid material via a radiation-sensitive material. Lithography is used to obtain different layers of material. During lithography, a photosensitive material is selectively exposed to a radiation pattern. The radiation then alters the physical properties of the material and enables the etching of the film. Etching removes the

sacrificial layers of material. Wet etching will dissolve the undesired material when immersed in chemical solutions. While dry etching dissolves, or sputters, the material uses reactive ions or a vapor as the etchant. The radiation used in this process may be optical, x-ray, electron beam, or ion beam. The most widely used form of lithography is photolithography, which utilizes optical exposure. Photolithography has matured rapidly and become useful at resolving smaller and smaller features. Photolithography consists of two basic steps: pattern generation and pattern transfer. The first step, pattern generation, begins with the generation of a mask through computer aided design. The mask is a stencil used to generate a desired pattern in resist-coated wafers and then repeated. A photomask, which is a nearly optically flat glass or quartz plate with a metal absorber pattern, is placed into direct contact with the photoresist coated surface and the wafer is then exposed to ultraviolet radiation. A light or dark field image is, therefore, transferred to the semiconductor surface. This procedure results in a 1:1 image of the entire mask onto the silicon wafer. The second step, pattern transfer, involves: (1) dehydration and priming of the surface, (2) photoresist coating of the wafer, (3) soft bake of the photoresist, (4) exposure of the photoresist through the mask, (5) chemical development of the photoresist, (6) wafer inspection, and (7) postdevelopment bake or hard bake. [2]

2. Etching

The process of etching is the pattern transfer from the photoresist, such as in a hard bake, to the underlying film or wafer. Etching is defined as the selective removal of unwanted regions of a film or substrate. It is used to delineate patterns, remove surface damage, clean the surface, and fabricate 3D structures. The two main categories of etching are wet-chemical etching and dry etching.

Wet etching is the removal of material by immersing the wafer in a liquid bath of the chemical etchant. Wet etchants fall into two broad categories. They are isotropic etchants and anisotropic etchants. Isotropic etchants attack the material being etched at the same rate in all directions. Anisotropic etchants attack the silicon wafer at different rates in different directions, allowing more control of the shapes produced. Depending on the concentration of the impurities in the silicon, some etchants attack silicon at different rates. "V" shaped grooves and chambers are the simplest structures and can be

formed using KOH, a wet etchant, to etch a silicon wafer with the most common crystal orientation (100) -- right angled corners and sloping sidewalls. Using wafers with different crystal orientations can produce grooves or pits with vertical walls. For dry etching, the most common form for micromachining applications is reactive ion etching (RIE). Ions are accelerated towards the material to be etched and the etching reaction is enhanced in the direction the ions travel. RIE is an anisotropic etching technique. Deep trenches and pits with vertical walls can be etched into a variety of materials including silicon, oxide and nitride. Unlike anisotropic wet etching, RIE is not limited by the crystal planes in the silicon. The term "Deep" is often added so the technique may be referred to as DRIE. These three basic sequences are applied differently in each fabrication technique. [2]

3. Bulk Micromachining

Bulk Micromaching was the first IC technology developed in 1967 and has since been refined to develop the MEMS construction techniques. In Bulk Micromachining, large portions of the substrate are removed to form the desired structure. Because thicker substrates can be used with this method of fabrication, deep or tall structures can be formed. Figure 2-2 demonstrates the crystal plane shapes and the basic two step process.

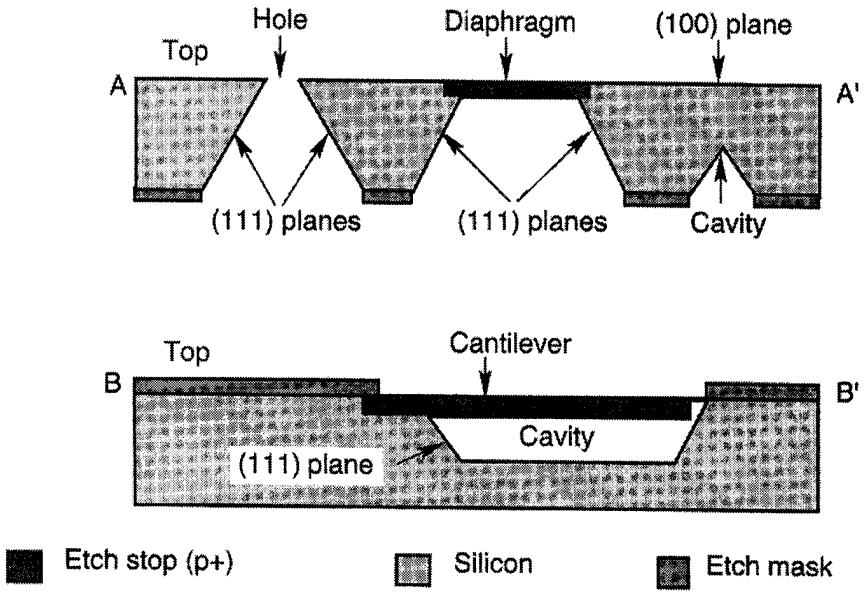

Figure 2-2. Simple MEMS Bulk Manufactured Beam [From 2]

4. Surface Micromachining

Surface micromachining enables complex, multi-component, integrated micromechnical structures that are unobtainable through bulk micromachining techniques. This method requires a continued process in which structures are built layer by layer, on the surface of the substrate. The substrate is employed as a mechanical support and remains mostly untouched. The alternating layers of structural and sacrificial material create the micromechanical structures. [2]

This process would typically employ films of two different materials, a structural material and a sacrificial material, usually oxide. These are deposited and dry etched in sequence. Finally, the sacrificial material is wet etched away to release the structure. The more layers, the more complex the structure, and the more difficult it becomes to fabricate. The maximum thickness of a polysilicon and silicon dioxide (SiO_2) micromechnical device is limited to 10 μm due to the residual stress in the thin film layers. [2]

A simple surface micromachined cantilever beam is shown in Figure 2-3. In this figure, oxide is the sacrificial layer and is deposited on the surface of the wafer. A structural material layer of polysilicon is then deposited. This layer is then patterned using reactive ion etching (RIE) techniques, to a beam with an anchor pad as shown in Figure 2-3(b). Figure 2-3 (c) shows the layer before wet etching. Figure 2-3(d) shows the wafer wet etched to remove the oxide layer under the beam. The anchor pad has been under-etched. The wafer is taken from the etch bath once all the oxide is removed from under the pad, thus leaving the beam attached to the wafer. [2]

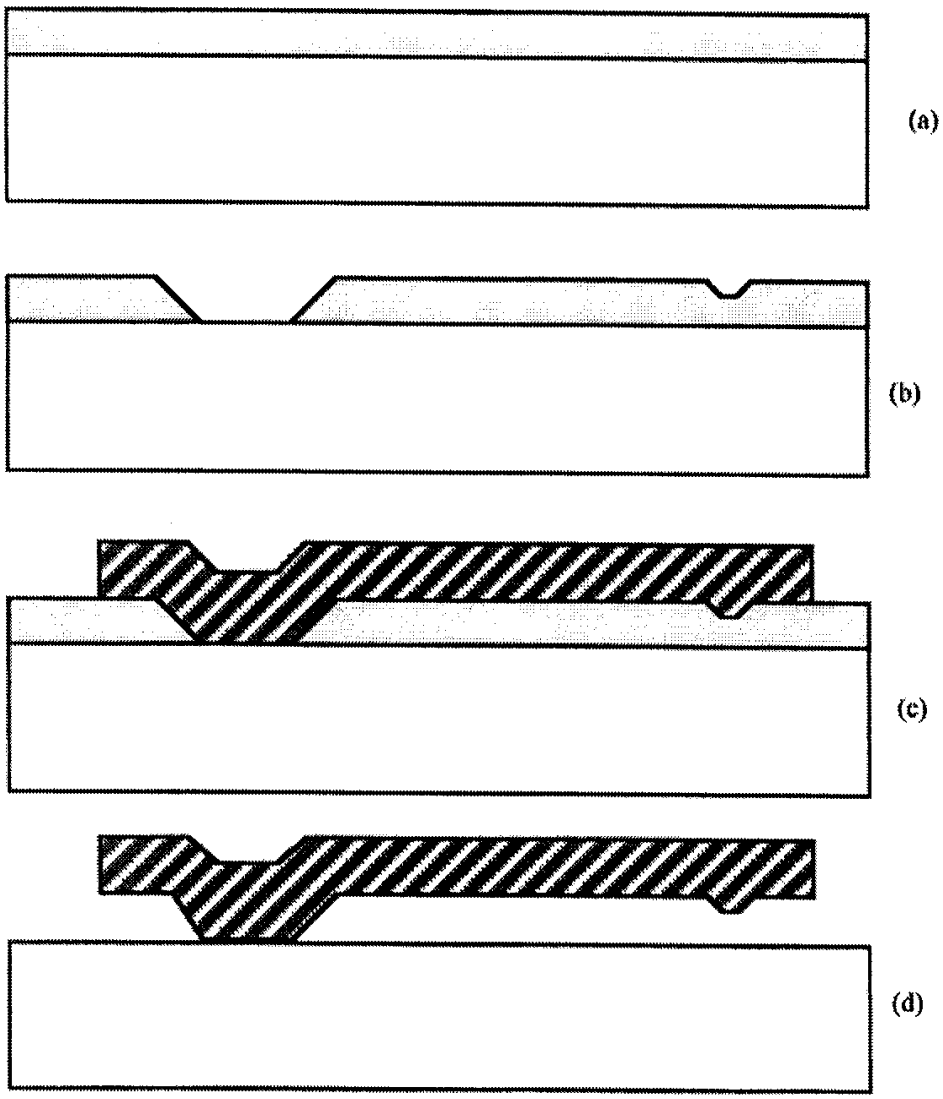

Figure 2-3. Schematic of a Simple Surface Micromachined Cantilever Beam [From 2]

5. Excimer Laser Fabrication

Excimer lasers produce relatively wide beams of ultraviolet laser light. Unlike other types of lasers, excimers do not remove material through excessive thermal energy - they vaporize it. As a result, the material adjacent to the area machined is not melted or distorted by heating effects. The strength of an excimer laser is its use in micromachining of organic materials such as plastics and polymers.

The laser is pulsed on and off removing material with each pulse when machining organic materials. The amount of material removed is dependent on the duration of the

pulse, the material itself, and the intensity or fluence of the laser light. Depending on the material, below a certain fluence threshold, the laser light has no effect. As the fluence is increased above the threshold, the depth of material removed per pulse is also increased. It is, therefore, possible to accurately control the depth of the cut by counting the number of pulses. Thus, deep cuts can be made using the excimer laser. Using a chrome on quartz mask, like the masks produced for photolithography, controls the shape of the structures produced. The mask is placed in contact with the material being machined, and the laser light shines through it. A more complicated and versatile method involves projecting the image of the mask through a lens onto the material. Material is selectively removed where struck by the laser light. [2]

6. LIGA (Lithography, Electroplating, and Molding)

LIGA utilizes a lithography, electroplating, and molding processes to produce microstructures. This process creates finely defined microstructures up to 1000 μm high. A unique type of photolithography employing X-rays is used to produce patterns in very thick layers of photoresist. The X-rays from a synchrotron source shine through a special mask onto a thick photoresist layer, which is sensitive to X-rays. This layer covers a conductive substrate as shown in Figure 2-4. Figure 2-4 (b) shows this resist developed. The pattern formed is then electroplated with metal in Figure 2-4 (c). The metal structures produced can be the final product. It is common, however, to produce a metal mold in Figure 2-4 (d). This mold can then be filled with a suitable material, such as a plastic Figure 2-4 (e), to produce the finished product (see Figure 2-4 (f)). [2]

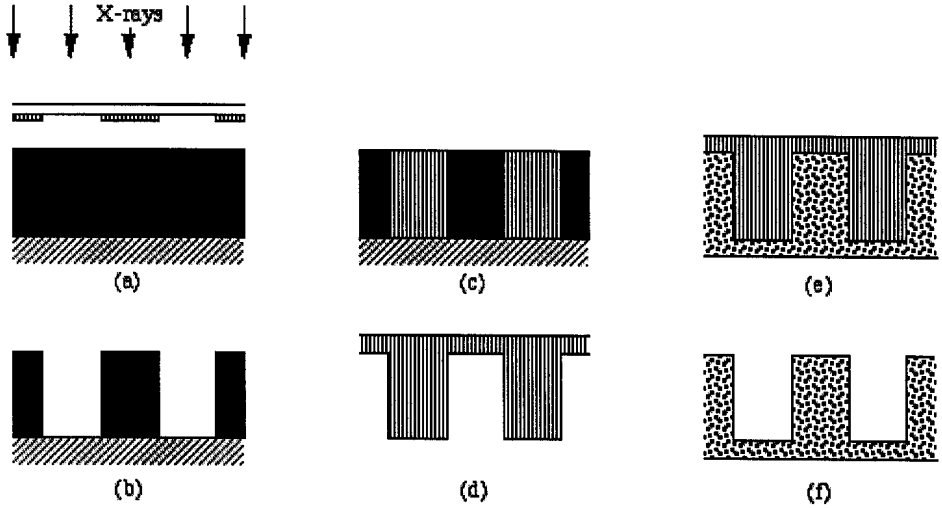

Figure 2-4. LIGA Micromachining Techniques. [From 2]

THIS PAGE INTENTIONALLY LEFT BLANK

III. ASTRONAUTICAL APPLICATIONS

The purpose of this section is to provide the engineering science associated with spacecraft design. The main focus is on the propulsion subsystem and other subsystems are covered only as they apply to propulsion.

A. ASTRODYNAMIC BACKGROUND

Satellite positioning is a parameter that directly influences the propulsion system requirements. The propulsion system places a satellite into a specific orbit or trajectory and ensures that it maintains course and speed. The stability of the satellite is controlled either by onboard computer processing equipment or from a stationary ground facility.

1. Notation

The orbital parameters shown in Figure 3-1 and 3-2 demonstrate notation used to define and control satellite orbital position. All natural space bodies follow principles of ballistic motion. The propulsion system is used as needed to meet mission requirements. Very few satellites have a propulsion system that operate continuously throughout their mission. The application of Kepler's 3rd Law is especially useful to orbital mechanics where:

$$T^2 = \left(\frac{4p^2}{mM} \right) (R + z)^3 \qquad (3\text{-}1)$$

T = period of one revolution, μ = central body gravitational constant (Earth's is 3.986 x10^5 km/s^2), M = mass of the earth, r=earth radius, z=satellite altitude.

Kepler's 2nd Law states that an orbiting body follows an elliptical path where one of the foci is the main gravitational body, e.g. earth. In Figure 3-1, this is point F.

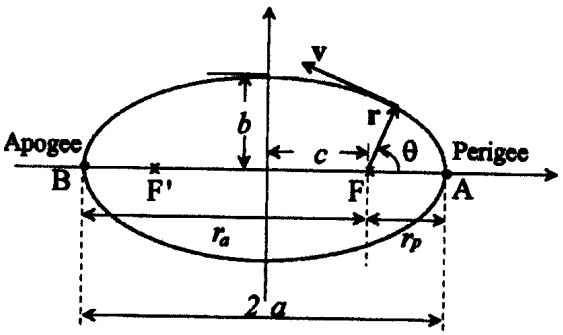

Figure 3-1. Two Dimensional Elementary Orbit [From 4]

Also shown in Figure 3-1 is the apogee (high point of orbit, B), perigee (low point of orbit, A), the major axis (2a) and the minor axis (2b), the satellite altitude at apogee is r_a and at perigee r_p, the orbital velocity (v), the current satellite altitude (r), and the satellite's current position (true anomaly, θ). It is important to notice that a circular orbit is a specialized elliptical orbit where the major and minor axis are equal, apogee and perigee are equal, and the main gravitation body is the only focal point.

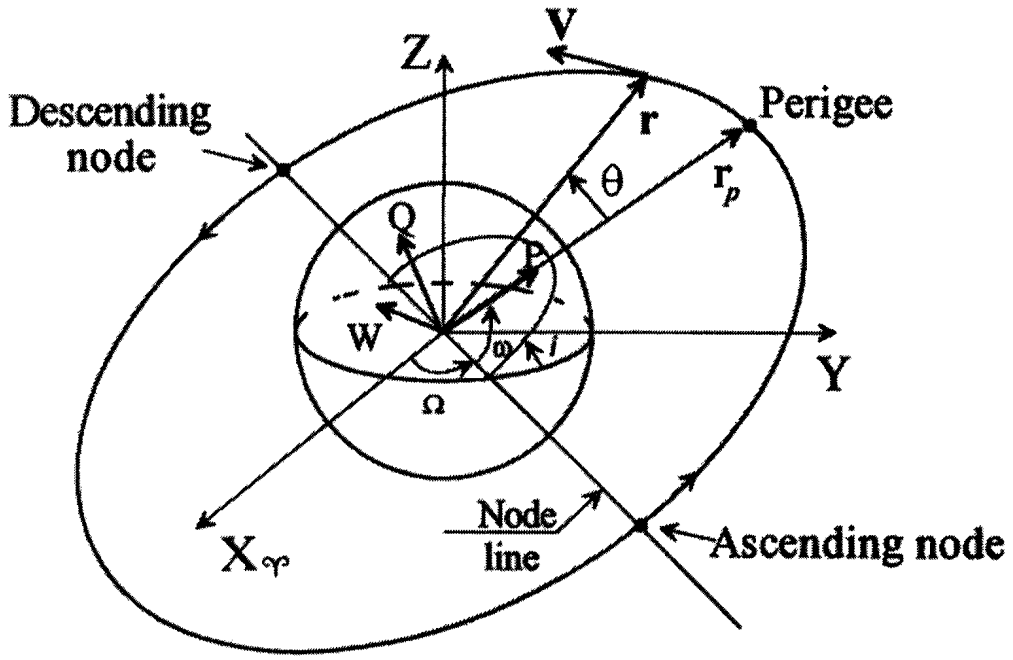

Figure 3-2. Three-Dimensional orbit diagram with Celestial Coordinates [From 4]

In addition to the basic notation shown in Figure 3-1, Figure 3-2 reveals the increased complexity which occurs in orbital design when moving from a two dimensional orbit to a three-dimensional orbit. There are two distinct reference frames: the celestial reference frame, (X, Y, Z) and the satellite terrestrial reference frame (P, Q, W,). Further notation used in Figure 3-2 is: the Inclination (i) - angle orbit makes with equator; ascending node - equator crossing position moving northward; descending node - equator crossing position moving southward; eccentricity – shape or departure from circular (ellipse); argument of perigee (ω) – angle from the ascending node; longitude of ascending node (Ω) – angle of ascending node from galactic point Vega (♈).

2. Orbital Drift

Many forces affect the flight path of a spacecraft and alter its motion from the Keplerian predictions. Without a propulsion method to provide corrective changes, the satellite would not be able to maintain a stable orbit and continue its mission. These influences are referred to as perturbations, or deviations in all orbital elements from normal idealized motion. The two categories are short term and long term. The diurnal forces, short term, are daily changing forces affecting orbital periods. Secular forces are long term perturbations that are apparent only after weeks of observation. The five major perturbations affecting spacecraft: (1) the argument of perigee and angle of the ascending node moves as a result of variations in the earth's gravitational field. Specifically the earth is an elliptical spheroid, with an equatorial "bulge", and the resulting perturbation must be accounted for in mathematical modeling methods. (2) The gravitational effects of third body influence a satellite's orbit, especially the high earth orbits. (3) Atmospheric drag, which exists in the lower orbital altitudes. The atmosphere affects spacecraft out to an altitude of 850 km. (4) The electromagnetic field is not uniform and therefore induces asymmetric forces on a satellite, especially LEO satellites. (5) The solar wind and galactic bombardment are very small forces, but over long periods of time they do affect the satellite's orbit. [4]

3. Orbit Definitions

Figure 3-3 depicts the three main orbit classifications. High earth orbits (HEO) tend to be highly elliptical. Russia was the first country to effectively utilize satellites in these orbits to accommodate their northern launch sites and geography. Thus highly

elliptical HEO are referred to as Moylnia Orbits. HEO altitudes are over 36,000 km. Geosynchronous (GEO) are special orbits with a period matching the Earth's rotation of 24 hrs. A special class exists for GEO satellites with in equatorial orbit, these satellites remain over one spot on the earth at all times. The altitude of GEO satellites is 35,780 km. Deep space refers to satellites beyond the GEO altitudes. Mid earth orbits (MEO) are between 800 km to 30,000 km altitude. Low Earth Orbits (LEO) are very low orbits, below 800 km and tend to be circular. Although one of the harshest space environments is near the earth, there are many communication satellites and weather satellites within this region of electromagnetic hazards. [4]

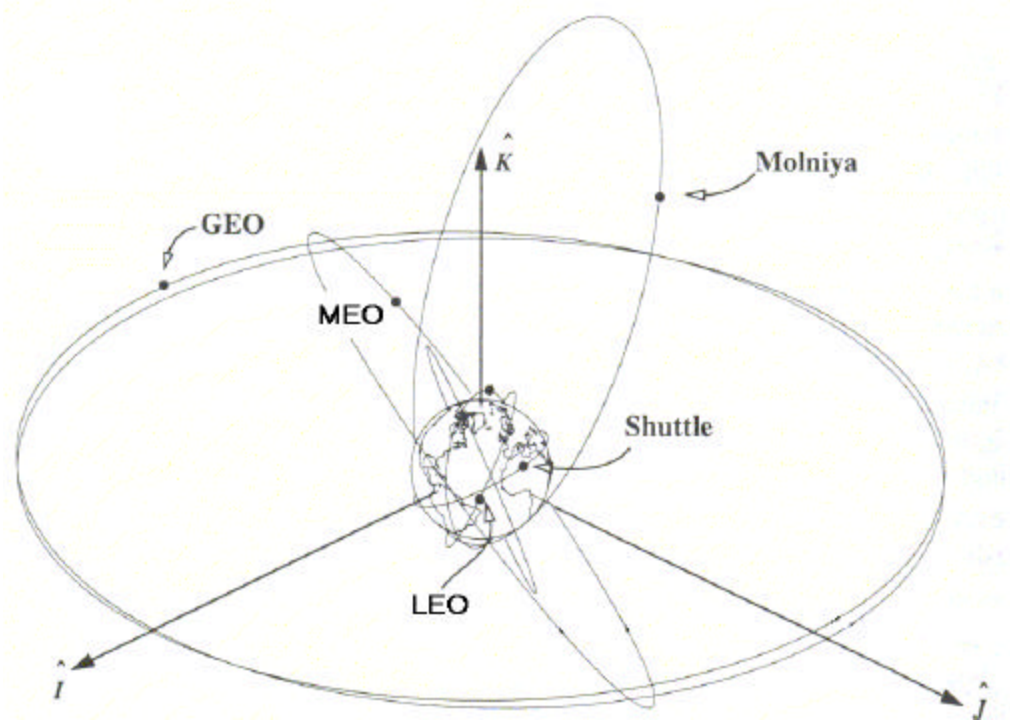

Figure 3-3. Satellite orbits with i, j, k reference frame [After 4].

B. ORBITAL MAINTENANCE

Propulsion systems impart the energy to the spacecraft enabling it to perform, or maneuver, while on orbit. Additionally, most satellites are required to have a "de-orbit" capability to prevent the accumulation of dead satellites and extra "space debris". A de-orbit propulsion system is used to push the satellite into a lower orbit, and subsequently burn up on re-entry into the earth's atmosphere. Large satellites that are unable to be completely destroyed on re-entry are required to use their propulsion system to raise their

orbit to a very high altitude where they will not interfere with other satellites. The three maneuvering classifications are orbit changes, station keeping, and attitude control.

1. Orbit Changes

Initial orbit raising and lowering typically occur at the mission start and mission end. Once the launch vehicle places a satellite in its initial orbit, the satellite provides the energy to reach its final mission orbit. The most commonly used methods are either a single use apogee kick motor (AKM) to rapidly complete the orbital maneuver, or slowly with multiple usage of a main thruster. The slow method consumes less fuel which in turn reduces the launch vehicle requirements. The slow and steady orbital maneuver is ideally suited for electric propulsion. The amount of energy required can be predicted by applying Kepler's 3rd law (equation 3-1). Using the same nomenclature, the velocity required to maintain a specified altitude is:

$$v = \sqrt{\frac{2m}{r} - \frac{m}{a}} \tag{3-2}$$

There is a velocity difference between two different orbital altitudes and therefore a difference in kinetic energy. However, the potential energy present in a higher orbit means that a higher orbit has more total energy than a lower orbit. The propulsion system also imparts the energy required to change the inclination, eccentricity, or any of the other components of the complex orbit. [4]

2. Station Keeping

Station keeping is the ability of a satellite to remain within an orbital window. The ground station receives information from the satellites and provides the command input to control and maintain satellite position. In satellite formations, the ability to maintain physical separation is crucial to mission success. North-south station keeping is the latitude control of the satellite. The east-west direction is the longitude control. A special situation exists for GEO altitudes where station keeping is a zero thrust problem and the satellite maintains a relatively fixed position. The resulting ground track is a figure eight. [4]

3. Attitude Determination and Control

The two aspects of the Attitude Control System (ACS) are how to control the satellite and how to determine if the satellite is stable. How the satellite is stabilized is a considerable aspect of the design process. The three basic types of satellite control are no control, a tumbler, a spin-stabilized satellite, like a spinning top, and a 3-axis stabilized satellite, which is typical of many satellites. The method used to maintain 3-axis stabilization is another complicated aspect of satellite design. Satellites can be controlled with torque rods, momentum wheels, or thrusters. Torque rods generate a reaction torque by applying an electric current across the earth's magnetic field (**j** x **B**). This is effective only in LEO. The earth's magnetic field is too weak in higher orbits. Momentum wheels are relatively large masses that resist movement in accordance with inertia, or conservation of momentum. In a small satellite extra mass must be avoided. The thruster system applies a force in each direction, as shown in Figure 3-4. This is the least complicated thruster arrangement and requires 16 thrusters. The total number of thrusters can be reduced to four if each one is precisely angled and if a good computer system is onboard to process the required algorithms. [5]

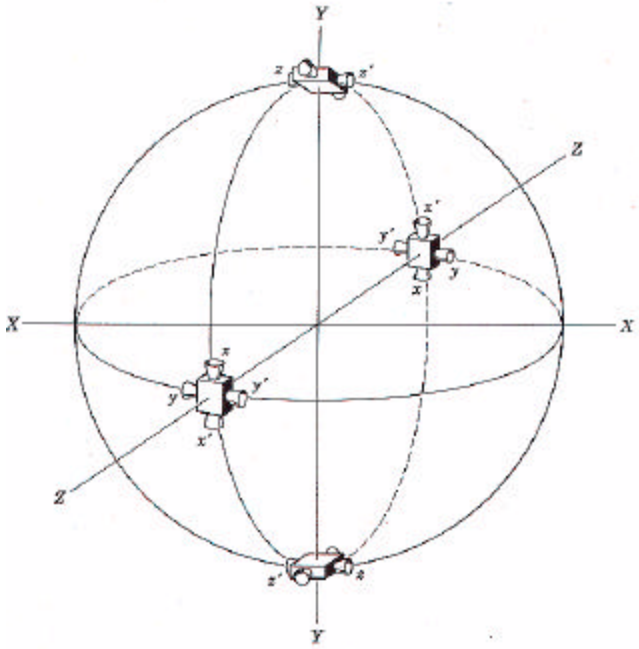

Figure 3-4. Thruster Arrangement for Attitude Control [From 6]

C. THRUST GENERATION

Thrust generation is the fundamental goal behind a propulsion system. Recalling the conservation of momentum, the thrust in rockets is produced by discarding propellant mass. This mass ejection generates thrust according the elementary rocket equation where thrust (F) is the product of mass ejection ($\dot{m}$) and velocity (v). Obviously to generate more thrust requires either more mass or a higher exit velocity.

$$F = \dot{m}\mathrm{v} \tag{3-3}$$

The goal of propulsion optimization is to eject the propellant at the highest possible velocity and minimize the propellant mass losses. The measures of performance for rockets are thrust and specific impulse (I_{sp}). [6]

Specific Impulse is thrust divided by the mass-flow-rate of propellant through the thruster, and is a function of propellant and thruster type.

$$I_{sp} = \frac{F}{\dot{m}g_0} \tag{3-4}$$

I_{sp} is a performance measurement similar to an automobile's miles per gallon, the higher the better. Higher I_{sp} means that less propellant is required to perform a given mission. An associated term is the minimum impulse bit, which is the smallest value of the time integral of thrust a given propulsion system can deliver. For the minimum impulse bit, the smaller the better, especially for propulsion systems used for attitude control.

The start of modern rockets began with the steam engine and the convergent nozzle. During the late 19^{th} century, a Swedish engineer of French ancestry, Gustav DeLaval, realized that the convergent nozzle limited the exhaust velocity and in order to get more energy out of the nozzle, the nozzle must first converge and then diverge. The DeLaval nozzle is shown in Figure 3-5. All modern thrusters use a convergent/divergent nozzle to expand propellant in a plenum at pressure (p_1) and temperature (T_1) to a much lower ambient pressure (p_2). Some forms of electric propulsion do not use these nozzles, like pulsed plasma thrusters and Hall thrusters. Converting propellant enthalpy into directed kinetic energy creates thrust. The converging section accelerates the flow until

the flow velocity reaches the throat at sonic speeds, Mach 1. After this point, a diverging section is required for continued expansion of the gases, continued increase in velocity, and subsequently an increase in the thrust.

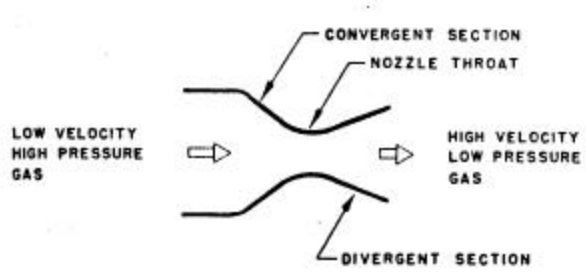

Figure 3-5. The DeLaval Nozzle [From 7].

The theoretical specific impulse for these gas-dynamic thrusters is given by the following equation: [6]

$$I_{sp} = \left(\frac{1}{g_0}\right)\left\{\left[\frac{2kR'}{(k-1)}\frac{T_1}{MW}\right]\left[1-\left(\frac{p_2}{p_1}\right)^{(k-1)/k}\right]\right\}^{1/2} \qquad (3\text{-}5)$$

The definition of terms used are: gas temperature (T_1), gravitational acceleration at Earth's surface (g_0), ratio of specific heats for propellant in the reaction chamber (k), universal gas constant (R') (8,314 J/mol-K), molecular mass of the exhausted gas (MW), chamber pressure (p_1), and pressure at the exit plane (p_2).

From an analysis of equation (3-5), I_{sp} can be increased by increasing chamber temperature (T_1), decreasing the molecular mass of the exhausted gas and the ratio p_1/p_2 can be increased. Usually, temperature is increased using chemical reactions and/ or electric heaters. Low molecular mass (MW) propellants like hydrogen, water or ammonia are used for externally powered thrusters. It is important to note that this equation is purely thermodynamic, and physical scaling does not enter into the simplified theoretical calculation of specific impulse. [6]

IV. MICROTHRUSTER TECHNOLOGY

As MEMS are incorporated into existing space applications, a technological challenge is to adapt various propulsion features into the realm of microthrusters. The need of micropropulsion has been established. This section presents several options available to ensure the propulsion system meets mission requirements. Many of the new propulsion architectures based on MEMS fabricated devices exist but require additional experimentation and study before they can be properly utilized.

A. PROPULSION OVERVIEW

The different propulsion systems available for microthruster technology is presented in an organizational table, Table 4-1, according to common features.

Class	Thruster Type	Specific Impluse [sec]	Thruster Efficiency [%]	Dry Mass [g]	Thrust [mN]	Technological Issues
Chemical	Cold gas	40-80	95+	100-500	5-1,000	Drag losses at low Reynolds numbers, Propellant storage requirements to minimize leakage.
	Mono-propellant	80-290	95+	100-500	1000+	
	Solid-proplellant	100-290	75-90+	2-1,600	50-100	Ignition reliability
Electrical	Resistojet	150-330	18-40	~800	1-6	Drag losses and propellant storage.
	Hall Effect thruster	500-1500	5-40	1,000-1,600	1.8-13	Plasma containment, Propellant storage requirements to minimize leakage.
	Colloid Ion Engine	500-1500	50-75	500-1,600	0.4-1.4	
	Pulsed Plasma Thruster	800-1000	2-12	80-500	0.002-0.1	Fuel Geometry, Ignition source.

Table 4-1. Micropropulsion Systems with Technology Issues. Estimated dry mass will vary to accommodate propellant requirements. Data obtained from references 2, 6, 9, 10, 11and 24.

Although readily apparent, not all conventional thrusters can be effectively scaled down to MEMS-size levels. Cold gas, monopropellant, resistor-jet, and solid propellant thrusters can and have been scaled down to milli-newton thrust levels but at the expense

of reduced performance arising from viscous losses. There are limits on how small nozzles can become and still remain effective. Bi-propellant systems have a physical limit on how small the combustion chamber can be. The chamber volume must be large enough to allow the gaseous propellants to mix and complete the combustion process. Efficiency is a factor in the liquid to gas phase change, the oxide and fuel mixing ratios, and completeness of combustion. The fundamental bimolecular reaction rates dictate the necessary reaction area and chamber volume. Two electric propulsion systems: ion engines and Hall-effect thrusters are also difficult to reduce in size because the magnetic confinement does not scale linearly with size. For all systems, except the Pulsed Plasma Thruster, a significant scaling problem is propellant leakage difficulties associated with valve miniaturization. Traditional metals are difficult to machine to the microscale and MEMS technology utilizing glass or silicon are very porous to gaseous propellants - exceeding acceptable leakage rates.

B. COLD GAS MICROTHRUSTER

All of the components used in the cold-gas system are also used in other chemical thrusters. Thus scaling success and difficulties associated with a cold gas thruster will impact other thrusters. The nozzle, an essential component of all thermal propulsion architectures, requires proof of design to lead the way for the micro-chemical systems. There are many advantages to developing an effective micro-fabricated nozzle. Traditional pressurized propulsion systems suffer from high viscous losses at the low chamber pressures required for low thrust performance. Cold gas propulsion systems have the lowest complexity and cost of all the chemical systems. Cold gas systems are capable of providing highly repeatable, extremely small impulse bits for accurate orbit maintenance and attitude control but at the expense of specific impulse and total impulse for a given volume. Since miniature cold gas thrusters are able to provide small and precise impulse bits of thrust, they have become an acceptable option for attitude control and station keeping applications. [8]

1. Effects on Scaling

As previously stated, the DeLaval nozzle uses the convergent/divergent expansion to convert the enthalpy of the fluid into kinetic energy. Expanding the terms used in Equation 2-1, provides additional information on nozzle operation.

$$F = \dot{m}v_2 + (p_2 - p_3)A_2 \tag{4-1}$$

Where the thrust (F) is equal to the sum products of mass flow rate ($\dot{m}$), exit velocity (v_2), the exit pressure (p_2), the ambient (atmospheric) pressure (p_3) and the nozzle exit area (A_2). It is import to note the equation must be further simplified since in space the atmospheric pressure is effectively a vacuum (p_3=0). [6]

Using equation (4-1) it is apparent that the thrust can be adjusted by changing the mass flow rate and exit area. Unfortunately altering the exit area or exit pressure is not very effective. Thus the mass flow rate can be altered in order to adjust the thrust. Fluid dynamics provides this definition of mass flow rate within the nozzle:

$$\dot{m} = \rho A v \tag{4-2}$$

Where the symbols are density (ρ), applicable cross sectional area (A), and velocity (v).

Ideal gas dynamics show that $p = \rho RT$: the pressure is equal to the product of density, universal gas constant, and temperature. Which means, for a homogenous gas mixture at constant temperature, the pressure is directly proportional to density ($p \propto \rho$). Thus a reduced thrust can be by achieved by a reduction in chamber pressure. The sequence of relations is through properties of ideal gas and equation 4-2: if pressure is lowered then density is lowered; if density is lowered then the mass flow rate is lowered; and if mass flow is lowered then the generated thrust is less. Real gases follow the same relation as ideal gases, but not precisely and can not provide an exact solution. Additionally, another problem exists in space which makes altering chamber pressures a poor solution. In space there is a vacuum. Reducing the chamber pressure may result in the destruction of fluid flow and prevent proper operation of the thruster. The flow density is based on the molecular mean free path, the mean distance traveled by molecule

between collisions, which must remain smaller than the nozzle size. The validity of a continuum approach is a reflection of the Knudsen number (Kn). The Knudsen number is a ratio of the molecular mean free path to the size scale of interest. [9]

$$Kn = \frac{l}{L}, \quad and \quad l = \frac{1}{pd^2 n\sqrt{2}} \tag{4-3}$$

Where the variables used are: mean free path(λ), characteristic chamber size (L), average molecule diameter (d), number of molecules per unit volume in the gas (n). [9]

When the Knudsen number is greater than 0.1 (Kn > 0.1), the continuum fluid flow breaks down. To achieve smaller thrusts simply by reducing the chamber pressure will not work. A lower propellant chamber pressure requires a corresponding reduction in nozzle throat and exit areas to maintain continuum flow. There is a balance between chamber pressure and propellant density. If the density is insufficient, and the continuum flow is broken, then the fluidic kinetic energy will not reach Mach 1. Choking the propellant flow is a restriction of fluid flow to increase fluidic energy and is essential for supersonic nozzle operation. [9]

In a traditional large nozzle, deviations from ideal, or isentropic, flow are small over most of the flow chamber volume. Unfortunately in a smaller nozzle, the small size also results in higher flow anisotropy. The viscosity of real fluid is not the same as in ideal fluids. The primary cause of anisotropic effects is the boundary layer formation along the nozzle wall. Fluid flow along the nozzle wall creates a shear stress in the bulk fluid. The shear stress results in friction, which in turn reduces the fluid velocity. Figure 4-1 depicts the boundary layer formation along the diverging nozzle wall, where boundary layer thickness (δ) is determined from the local fluid density (ρ_∞), fluid velocity (V_∞), and distance (x). [9]

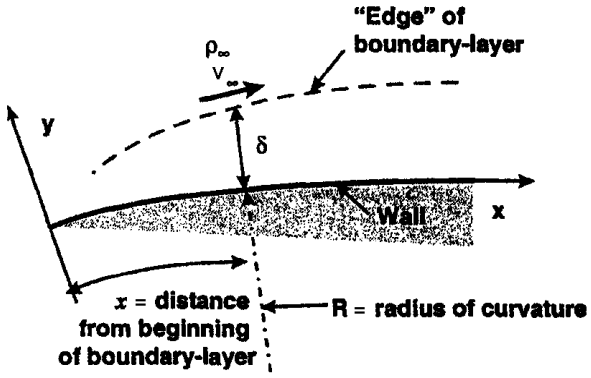

Figure 4-1. Boundary Layer Formation. [After 9]

$$\mathrm{Re} = \frac{r_\infty V_\infty L}{n} \tag{4-4}$$

The Reynolds number and the relationship between the boundary layer and the Reynolds number depend on the laminar or turbulent nature of the flow. Where the Reynolds number (Re) represents the relation between inertial and viscous forces within the fluid flow and is equal to the ratio of fluid viscosity (ν), density (ρ_∞), velocity (V_∞), and characteristic chamber dimension (L). [9]

In microthrusters, the boundary layer is likely a laminar boundary layer, such that the boundary layer has a slope (δ/x) inversely proportional to the Reynolds number ($\frac{\delta}{x} = \frac{1}{\sqrt{\mathrm{Re}}}$). Which implies that the boundary layer increases as the Reynolds number is decreased. The effects become pronounced as the boundary layer thickness increases and the nozzle cross sectional area is reduced in size. An endpoint is reached when the friction losses completely dominate the fluid flow and the boundary layer blocks the nozzle, preventing the gas flow from reaching sonic velocity. As the Reynolds number decreases the efficiency of a microthruster also decreases. MEMS research has established an optimized flat microthruster nozzle design: a throat width of 37.5 μm with an exit area to throat ratio (A_e/A_t) of 16.9:1, provides 10 mN of thrust at an I_{sp} of 65 sec. Numerical analysis simulations can be used to support demonstrated laboratory results. Figure 4-2 shows Mach contour lines of the MEMS thruster. In this figure the results use a chamber pressure (p_1) of 50 psia and Reynolds number of 1940 are shown. [10]

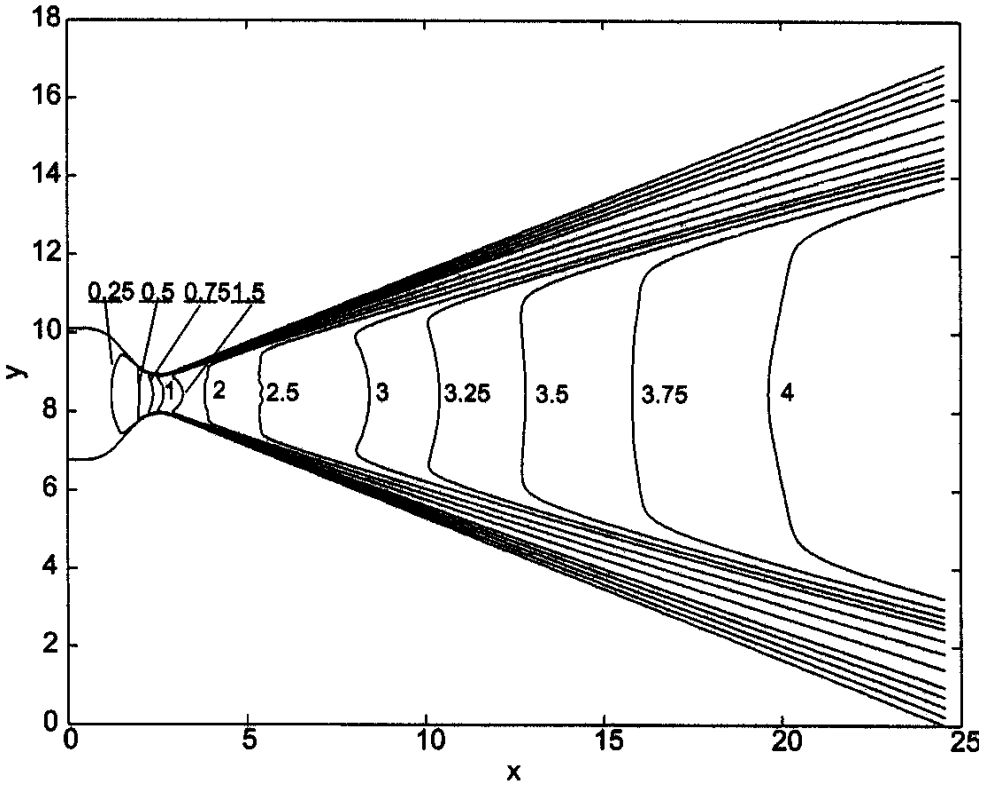

Figure 4-2. Mach contours of laminar flow in an optimized MEMS thruster. [From 10]

A MEMS fabricated nozzle is a flat nozzle, not conical. Figure 4-3 provides a comparison between circular and rectangular nozzles of the same cross section. The deep reactive ion etching techniques (DRIE) provide extremely small, and flat, nozzles. Traditional machining methods are not able to obtain a design of similar scale. Unfortunately, the flat nozzle is unavoidable due to MEMS fabrication methods and the advantages of micron-sized nozzles must be balanced against the increased surface area. As shown in Figure 4-3, there is a significant difference between the two *surface areas*.

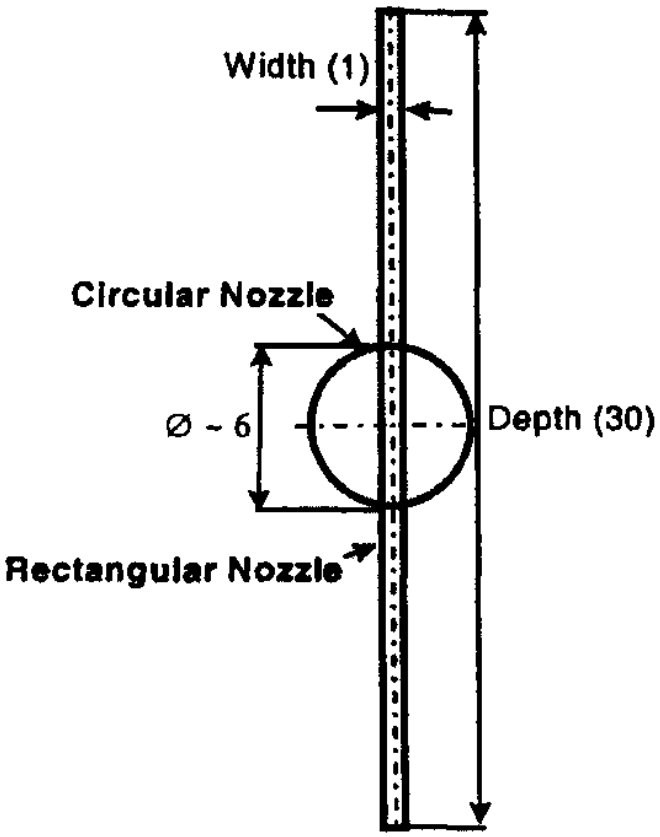

Figure 4-3. Unit-less size comparison between flat and round nozzles of equal cross sectional areas. [From 9]

2. Additional Problems

With low thrust levels and chamber pressure requirements, the MEMS cold gas thruster has a low I_{sp}, which leads to storage problems. For longer missions, leakage becomes a factor both in terms of attitude control and in terms of lifetime. For minor primary propulsion tasks and ACS functions with a relatively short mission duration and low overall impulse, cold gas systems may work well. The minimum obtainable impulse bits are on the order of 10 mN-s. With microspacecraft, the mission design impact of propellant leakage is amplified due to the limits placed on propellant quantity stored on the spacecraft. With a goal of decreasing spacecraft weight and mass propellant volumes shrink as well. The maximum allowable valve leak rates have to be adjusted accordingly to avoid the depletion of propellant before the end of mission duration. These leak rates have been estimated at values one to two orders of magnitude below rates available with current space-qualified valve technology. In addition, current MEMS valve technologies

are not space-qualified and exhibit leak rates higher than those found for state-of-the-art conventional space qualified valves. In this situation smaller is definitely not better. The smaller seating forces and sealing surface, a product of current MEMS technology, cause the excessive leakage rates. Significant additional development efforts in this area are a necessity. [11]

C. FLIGHT AVAILABLE THRUSTERS

There are currently very few space qualified microthrusters. This section covers the thrusters that have proven laboratory performance and have been incorporated into spacecraft mission designs.

1. Solid Digital Thruster Design

The Aerospace Corporation and JPL have established an interesting thruster called the digital microthruster. For short duration missions this is an ideal manner to include a controllable thruster. For orbit insertion, conventional solid propellants thrusters are commonly used. These thrusters are simple, reliable, and have high propellant density, giving high density specific impulse. The high density, easy storage, and relatively high performance make solid propellants a good candidate to perform primary propulsion on microspacecraft but the main disadvantage, similar to traditional solid propellant rocket motors, limits the thruster use to a single, high impulse burn for each thruster element used.

DARPA provided the funding to develop and fabricate a microsatellite digital thruster system. Digital propulsion consists of an array of single-shot thrusters that individually produce only one impulse each; spacecraft maneuvers are performed by firing unused thrusters at the right locations at the right times. Ten thousand thrusters can be created on a 10 cm^2 surface, using a center-to-center spacing of 1 mm. This thruster array is planar, scalable in area, does not require a propellant tank or microvalves. In addition to removing the leakage problem associated with MEMS gas storage, the rigid backplane can also be incorporated and function as a structural element. The array of microthrusters is highly redundant. The array can be programmed to fire individual thrusters, several thrusters at once, or in controlled sequences. Since the dimensions of

the individual rocket engines are under the designers' control, the creation of smaller and smaller impulse bits is a straightforward process. [12]

Figure 4-4. An Assembled MEMS Digital Thruster Array of 15 elements. [From 12]

Each array of small sealed plenums is constructed with a rupture diaphragm on one side. Each plenum is loaded with a fuel or an inert substance in gas, liquid or solid form. When it uses fuel, the fuel is ignited and reacts to form a high-pressure, high-temperature fluid. In the case of an inert substance, it is heated to raise its pressure. Once the pressure exceeds the burst pressure of the diaphragm, the diaphragm ruptures, and an impulse is imparted as the fluid is expelled from the plenum. Thus, each plenum can deliver one bit of impulse. The size of the impulse is determined during fabrication by the size of the plenum and the fuel that is loaded into it. This approach eliminates valves and, therefore, valve leakage. It substitutes one-shot, consumable, individual thrusters for a multi-use conventional thruster and fuel tank. The arrangement can be seen in Figure 4-5. Initial design testing used lead styphnate as the propellant. This propellant is a shock-sensitive explosive and is typically used as an initiator. Once triggered enough thermal energy exists to ignite a larger quantity of secondary propellant. This propellant arrangement has produced 0.1 mN-sec of thrust at 100 W applied to the polysilicon ignition resistor. It is anticipated that this can be increased by nearly a factor of 10 with more complete combustion of the fuel. [12]

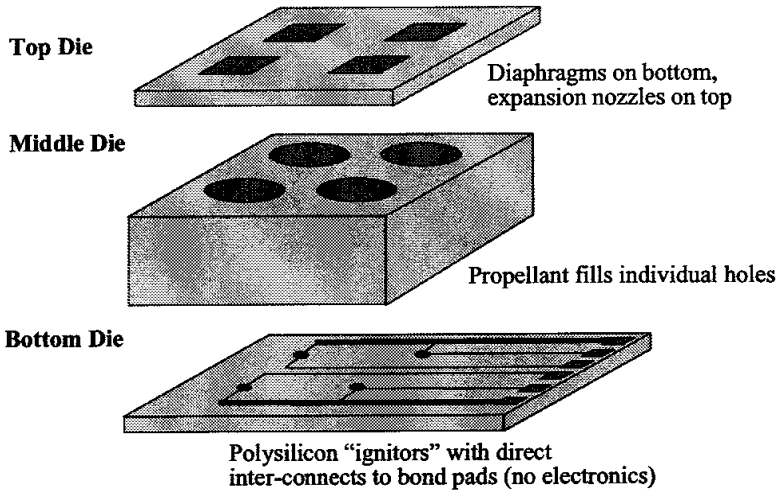

Figure 4-5. Current Digital Propulsion Configuration. [From 12]

2. Plasma Thrusters

As discussed in the following section, Section V, the Pulsed Plasma Thruster (PPT) was the first electric thruster and has a long history of space flight. Enabling technology has allowed significant improvements in thruster design. Towards that end a special section designated to address the PPT is included in the next section.

3. Cold-Gas Thruster

Current technology fails to allow an incorporated MEMS thruster. However the traditional machining methods enable very small thruster and valve construction. JPL has developed a system ready for space based testing. This option has a dry mass less than 1 kg.

D. EXPERIMENTAL THRUSTER OPTIONS

As technology enables increased miniaturization of propulsion components more options will be available to the spacecraft design. The laboratory experiments have determined the feasibility of the following thruster design options. Full implementation into an integrated spacecraft design requires additional work to overcome significant application defects.

1. Resistojet

Improvements to thruster performance by raising chamber pressure are apparent in equation 3-5. Raising the kinetic energy of the propellant gas increases the generated thrust. A resistojet is a heat exchanger integrated with a nozzle, resulting in a microthruster with an elevated chamber temperature. There are two different approaches to the MEMS scaled resistojet microthruster, sharing similar performance values and are equal in the development and testing process.

The Aerospace Corporation and JPL introduced a well-insulated version of a thin-film heater, a microresistojet using CMOS fabrication methods. The polysilicon resistor, deposited on a silicon substrate, is undercut through an anisotropic silicon etch. This defines the chamber as well as the nozzles, and leaves the heater suspended in the middle of the cavity such that the gas can flow across the upper and lower surface. Placing the heater centered within the chamber doubles the surface area of a conventional thin-film resistor, as well as reduces the thermal gradients across the chamber. [11]

A better design has been developed at MIT. This microresistojet design is significantly different with two key features that make it attractive for integrated micro-heat exchangers. First, the use of bulk silicon as both the structural and electrical material simplifies the system architecture and allows for high fluid/heater contact area. Second, the properties of silicon at the intrinsic point provide stable operation, particularly for gases where thermal runaway can be a problem. By increasing the chamber energy in a microthruster, the mass flow required for a given thrust level is greatly reduced. This translates into increased satellite life for a given propellant supply. Although the device efficiency is low in this initial example, little attempt has been made to minimize parasitic losses through the leads and test structure and one expects the efficiency could be improved in future designs. A second issue of concern in gas flow heat exchangers is heater stability which arise because the gas viscosity increases with temperature. If a local hotspot develops the fluid viscosity will increase, increasing the pressure drop across the heat exchanger passage, reducing the mass flow through the channel. Subsequently, cooling is reduced which raises the temperature in the channel. In this manner a thermal runaway occurs, leading to device failure. The microfabricated

solution achieves a highly effective heater in which the heater elements are formed from the structural material of the fluid system -- single crystal silicon. The two principal advantages of this architecture: the electrical and mechanical functions are combined and thermo-electric properties of silicon allow inherently stable operation at high temperature without risk of thermal runaway. The heater is used to increase the chamber temperature for fluid entering the micronozzle to create a propulsion system for a microspacecraft. The I_{sp} is improved by preheating the gas prior to expansion. Varying the number of passages, their length, thickness and spacing maximizes heater effectiveness. [13]

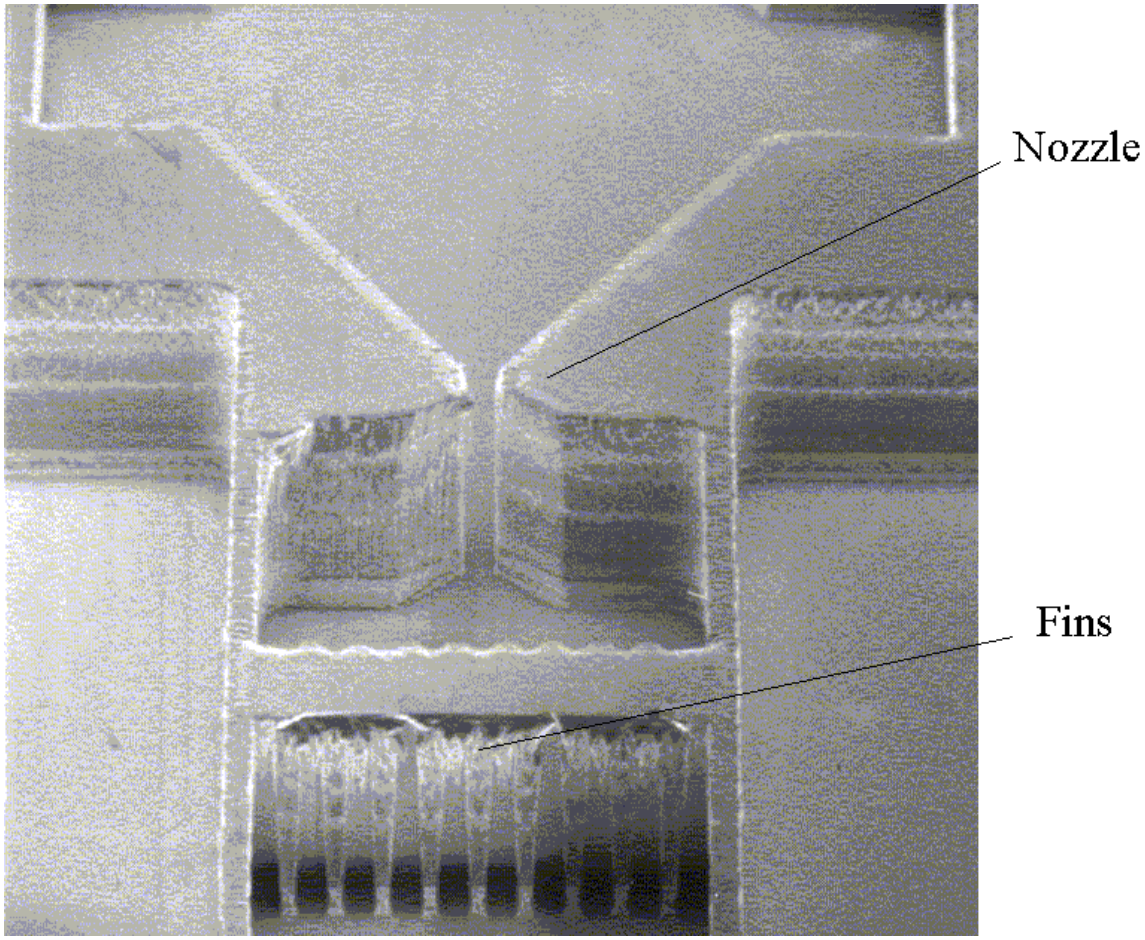

Figure 4-6. Image of Laboratory Resistojet design. [After 13]

The overall heater design is shown in Figure 4-6. Gas enters the port and flows through the heat exchanger, defined by narrow parallel fins upstream of the nozzle (bottom of picture shown in Figure 4-6). The structure is fabricated from heavily doped

P-type silicon. An electric current flows from top to bottom through the device, and is focused through the fins, heating them resistively. The properties of silicon as a semiconductor are used to maintain stable operation of the device at high temperature. By fabricating the heater using heavily doped P-type silicon wafers, the dopant holes will be the primary charge carriers at low temperatures. As power is dissipated and the temperature of the device increases, the electrons bound in the silicon valence bands become thermally excited to the conduction band. When the number of intrinsic carriers becomes dominant, the resistivity of the material decreases exponentially with temperature. The heater is operated in a constant current mode. As the current increases, the dissipated power, temperature, and resistance, all rise in response. However, when the intrinsic temperature is reached, any increase in dissipated power and temperature results in a resistance decrease. Consequently the dissipated power is reduced and the device returns to operation at the intrinsic point. Thus, a stable operating temperature is maintained with feedback provided by the resistive properties of silicon, a sensor intrinsic to the structure. [13]

With a heater design selected, the geometry, as shown in Figure 4-6, requires optimization to yield the highest heater effectiveness while maintaining the lowest pressure drop. Heat transfer in this instance is a convective transport problem governed by the bulk motion of the fluid. The fin width and the silicon resistivity determines dissipated power requirements. Heat is exchanged via convection transfer to the fluid and downstream portions of the fin. The heat transfer is dependent upon the fluid mechanics in the channel. Thus, the convection parameter is a function of Reynolds number and the distance along the fin. Since the heat transfer in the entrance region is high, all of the heat generated locally enters into the fluid. Heat generated downstream is conducted along the fin and enters the fluid where gradients are highest. The heater/nozzle system is fabricated in silicon using deep reactive ion etching (DRIE) methods. A halo mask is used to simultaneously outline the large cavities as well as define the small heater passages and nozzle throat. Matching these widths, a constant loading is maintained during the etch. In addition, a nested mask is used which allows the through wafer etch to proceed ahead of the heater-fins. This results in the heater fins being connected by a 50 μm high bus-bar, maintaining mechanical integrity and

providing electrical functionality. After etching, the cleared flow channels are encapsulated by fusion bonding silicon wafers to the upper and lower surfaces. Figure 4-6 is an electron microscopic image of the experimental 8.25:1 expansion ratio nozzle with a throat width of 65 μm, a nozzle depth of 491 μm. Although the I_{sp} is less than the theoretical value, it is 50% larger than that achieved with the cold gas flow. Thus the design trade is electrical power for propellant efficiency. This is an effective option since power can be renewable through solar arrays and propellant is not. The demonstrated propulsive efficiency of this device is quite low, 18%, primarily due to parasitic electrical losses in the electrical leads and test structure. However, with optimization of the design and better thermal insulation in the packaging, the efficiency could potentially be raised to 40%. [13]

2. Colloidal Ion Thrusters -- Field Emission Array (FEA)

This is an interesting electric propulsion system that uses MEMS technology to construct each element of the array and form a colloid thruster. Figure 4-7 is a drawing of one FEA element. An FEA consists of an array of conical tips placed opposite a gate electrode. Electrons are extracted from the tips accelerated in the electric field, and emitted through the aperture in the gate electrode. The sizes achieved with Silicon and Molybdenum are 2 nm for the tip diameter and 200 nm for the gate diameter. The achievable packing density is at least 10^8 tips/cm^2. Thrust is produced by electrostatic acceleration of charged liquid droplets ejected into the electric field generated between the tip and gate electrodes. It is this action of the applied electric field acting on the charged liquid droplets as they are extracted from the capillary apertures that produces thrust. [11]

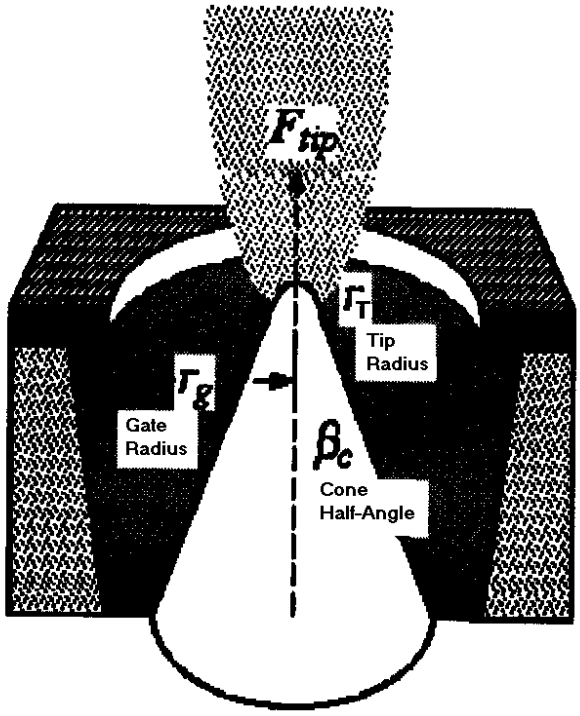

Figure 4-7. Conceptual Diagram of an FEA. [From 11]

Stanford University has tested a version of the FEA scaled for small satellites. The laboratory design has 100 capillary type emitter with an inner diameter of 50 μm. The gap distance between emitter and accelerator tip is 1 mm. The propellant is sodium iodine-seeded with glycerol. Test results yield 0.1 mN thrust at 1 W power levels with an I_{sp} of 500 sec. Total mass is 500 g with a volume of 100 X 100 X 200 mm^3. [11]

3. Resistojet -- Vaporizing liquid microthruster (VLM)

The vaporizing liquid microthruster is in the later laboratory design stage. A conceptual drawing is shown in Figure 4-8. Testing was suspended while an appropriate thrust stand was developed. The thrust stand was completed in the early part of 2002. The propellant is vaporized on demand at voltages between 2.2 - 4.3 V with power requirements ranging between 2.5 – 6.5 W. The generated thrust, between 0.1-1 mN with an Ibit between 10^{-7} and 10-^{5} N-sec, is produced by thermal expansion of the propellant vapor through a divergent nozzle. Many of the leakage problems associated with micropropulsion systems can be avoided by storing and using liquid propellants. Initial

testing has been with water, but future testing will include ammonia an possible hydrazine. [14]

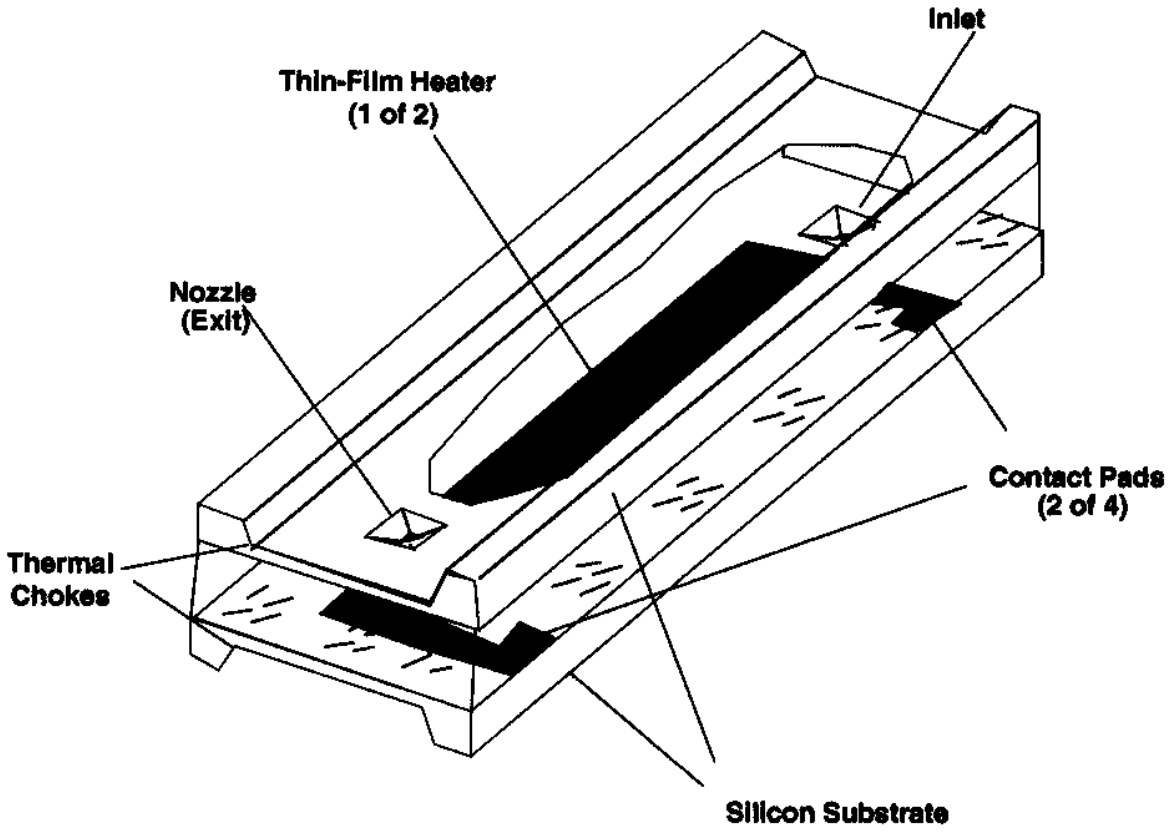

Figure 4-8. VLM DIAGRAM. [From 14]

4. Resistojet -- Free Molecule Micro-Resistojet (FMMR)

In a similar resistor jet to the VLM, the FMMR microthruster utilizes a fluid through a heater to generate a higher performance and higher density propulsion system. The heater is a thin film, resistively heated metal deposited on a silicon substrate. The heater is bonded into a plenum through which fluid flows, which is vaporized in the process. This is still highly in the development phase and needs more maturity for it to be a viable option for space propulsion.

The FMMR operates at very low exhaust pressures. The experimental design is arranged such that the exit surface is held at a stagnation temperature corresponding to a stagnation pressure between 50-500 Pa. The required spacing between the heating

element and the expansion slot corresponds to the mean free path of the stagnation gas. Maintaining an appropriate distance reduces intermolecular collisions that act to limit overall efficiency. In Figure 4-9, the variable "w" is the mean free path for the applicable propellant. The FMMR combines MEMS fabrication methods with lightweight materials to produce an option for space based thrusters. [11]

The optimized design has a slot length of 8 [mm] with a width of 100 μm and an expansion angle of 54.74 deg. With Argon propellant, a specific impulse of 45 sec and thrusts of 0.025 mN per slot were achieved. [11]

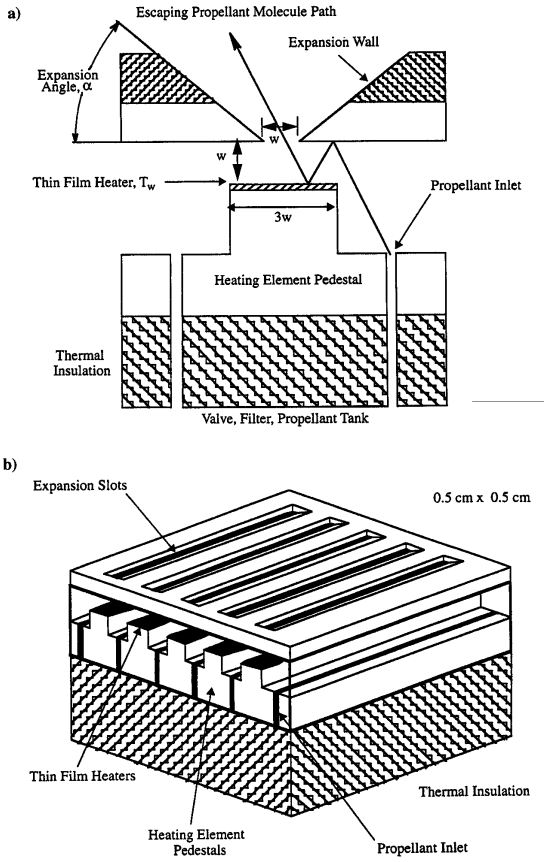

Figure 4-9. FMMR, a) side view b) orthogonal view. [From 11]

5. Laser Ablation micro-Thruster (LAmT)

With the advent of the highly reliable laser diode, this method of pulsed propulsion has become more than a possibility. When compared to other pulsed microthrusters, the minimum achievable impulse bits (estimated to be < 1 nNs) are lowest for the laser ablation microthruster. In general a laser is used to rapidly apply a large

amount of energy to a small area of propellant. With proper materials, the local binding energies are exceeded and a plasma is produced near the surface. The expanding plasma provides the thrust. [15]

A 1 W, 935 nm diode laser has been tested with a tape driven propellant feed system. The measured thrusts were 100 μN with a specific impulse between 100-1000 sec. Another experimental arrangement using a 1 W diode laser as a pumping source for a Nd:YAG microchip crystal operating at 1064 nm. The entire laser cavity is small enough to fit on the end of a standard fiber optic cable. The propellants are less limited and estimated thrusts of 3-300 μN were generated from aluminum, copper, stainless steel, indium and titanium. [15]

6. Vacuum Arc Thruster (VAT)

In this ablation thruster, a solid metal propellant is also the cathode. An inductively driven arc discharge generates spot temperatures which ablates the propellant and produces a metal-vapor plasma. Ion velocity can be as high as 30 km/sec. With tungsten propellant 12 μN/W thrust to power measurements have been achieved. The scaling ability of the VAC is tremendous. Power and pulse rates of 100 W and 200 Hz are achievable. The power plant unit can be as small as 100 g. [15]

Additional testing will prevent some of the problems encountered from reducing the reliability of the propulsion system. Specifically, there is a chance that an electrical short can occur between the anode and cathode and unlike Teflon®, there are difficulties in feeding a metal propellant between the electrodes. [15]

V. PULSED PLASMA THRUSTER (PPT)

A. HISTORY

Before space travel was ever considered, Faraday developed theories that relate to the electromagnetic thruster. The Pulsed Plasma Thruster (PPT) is a direct application of the Faraday accelerator, where mass ejection is due to the Lorentz force, a force acting on a current carrying conductor subjected to an external, perpendicular magnetic field.

The PPT was the first electric-propulsion system ever used onboard a spacecraft. In 1964 Russia used the PPT for attitude control and stabilization on the Zond 2 spacecraft mission to Mars. The United States waited until 1968 to apply PPT technology for the attitude control system (ACS) onboard the LES-6 satellite. The technology has continued to develop thus enabling PPT applications in spacecraft design. The simplicity and ruggedness inherent in the design of the PPT has encouraged research efforts to improve its extremely low thrust efficiencies.

The PPT operates with discrete impulse bits of thrust, allowing for the minute thrusts required for precise attitude control. The PPT has the following additional advantages: there is no warm-up time required prior to operation; it is able to be launched from a naturally inert state of charge; it is linearly scaleable for the desired spacecraft thrust; it is able to withstand rotations for dual-spun and three-axis stabilized spacecraft thrust vector control; and its variable thrust is compatible with digital commands. The propellant of choice is Teflon® $[C_2F_4]_x$. Teflon® has all the advantages of a solid propellant being stable, non-toxic, non-corrosive, also having a long shelf life, no storage tanks, no mechanical valves or feed lines, vacuum compatible, and remains unaffected by rapid accelerations or temperature changes. Other types of propellant have been evaluated and tested, but Teflon® remains superior. The primary disqualifier for most other plastic polymers has been excessive surface charring and/or a reduced I_{sp}.

With a stable solid propellant, an electric spark (or arc) is used to initiate the plasma. A plasma is a mixture of charged particles that conducts electricity, typically being above 5000 K. Electromagnetic thrusters accelerate the high temperature

propellant while an electric current flows through it. The traditional PPT uses a rectangular, breech fed propellant, and an LRC (inductive-resistive-capacitive) pulse circuit. (Figure 5-1). Having exposed a Teflon® bar to an electrical arc, the heat transfer from the arc causes ablation of the propellant and generates a plasma burst or “bit” of positively and negatively charged particles (in this case Carbon and Fluorine). The current is carried primarily by the free electrons which are electromagnetically driven between the cathode and anode "rails" that direct the plasma along the thrust chamber. The resultant thrust is generated by the burst of mass at its exit velocity. No propellant feed or regulation system is required as a simple spring mechanism advances the bar into the thrust chamber after each pulsed evaporation. Other PPT designs use a gas burst at the discharge electrodes which are more complex because of the propellant management requirements.

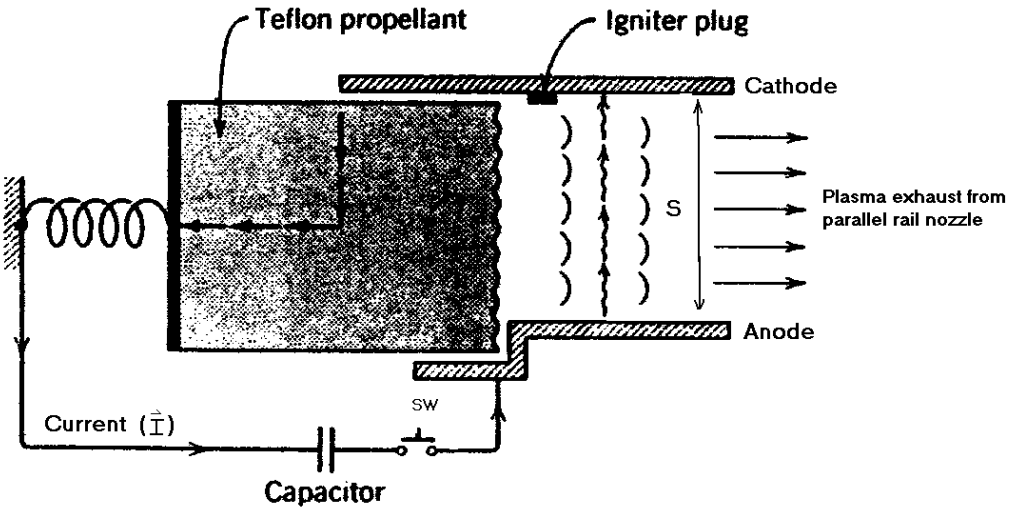

Figure 5-1. Breech Fed Rectangular Geometry PPT. [After 16]

The simple rectangular, breech fed geometry can be altered to include a "side-fed" system that uses two propellant bars which are advanced from opposite sides into the thrust chamber. In addition to the rectangular geometry, a coaxial geometry uses the same breach or side fed arrangements, (Figure 5-2). [16]

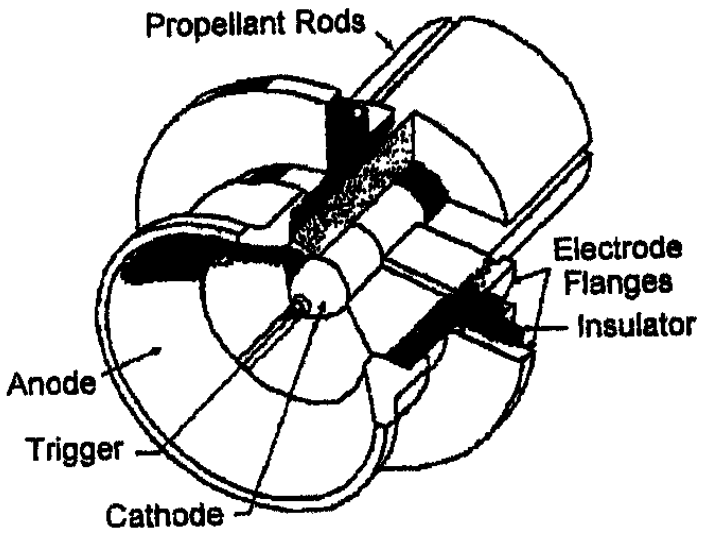

Figure 5-2. Breech Fed Coaxial Geometry PPT. [From 16]

B. MODELING/OPERATIONAL THEORY

With a PPT, the external magnetic field is induced by the electric-current loop formed by the charged rails, the discharge capacitor and the plasma. In a typical rectangular PPT as shown in Figure 5-1, significant components are: the distance between the charged rails, s, the total current, I and the induced magnetic field, B. In this arrangement the accelerating force acting upon the mass being ejected can be determined as follows: $\mathbf{F} = I(\mathbf{s} \times \mathbf{B})$. Thus the ejected mass accelerates at a rate of: $\mathbf{a} = I(\mathbf{s} \times \mathbf{B})/m$. Unlike a convergent/divergent thermal thruster, no change in area of the thrust chamber is required. One of the principal factors reducing system effectiveness is clear, the induced or opposing electromagnetic field (emf) developed by the moving charges, $\mathbf{v} \times \mathbf{B}$. When the plasma has accelerated to a speed where locally $E - vB = 0$, the main driver of the current vanishes. The plasma may still accelerate due to pressure gradients but not as vigorously.

In a PPT, the basic equations can be very complicated even though the physical components are not. The Magnetic Plasma Dynamic (MPD) equations can be applied to describe the electromagnetic thrust component. Ohm's Law ($\mathbf{j} = \sigma \mathbf{E}$) which is generalized below and the electromagnetic or Lorentz force ($\mathbf{j} \times \mathbf{B}$) are effective ingredients in the acceleration mechanism of the electromagnetic force. In a plasma field, with a high degree of ionization, the corresponding equations are:

$$\mathbf{j} = \sigma \mathbf{E}^{*} - \omega\tau(\mathbf{j} \times \mathbf{B})/B \qquad (5\text{-}1)$$

$$\mathbf{E}^{*} = \mathbf{E} + (\mathbf{v} \times \mathbf{B}) + (1/en)\nabla p_e \qquad (5\text{-}2)$$

$$P_E = \mathbf{E} \bullet \mathbf{j}, \; W_C = 1/2 \; CV^2 \; , \; W_L = 1/2 \; LJ^2 \qquad (5\text{-}3)$$

Where **j** is current density vector, σ is the scalar conductivity, **E** is electric field vector, **B** is magnetic induction (or magnetic strength) vector, **v** is the mass velocity vector, e is electron charge, n is electron number density, p_e is electron pressure, $\omega\tau$ is the Hall parameter (ω is the cyclotron frequency and τ is the mean time between collisions), and P_E is the electromagnetic power. W_c and W_L are the capacitor and inductor energies respectively.

Equations can only provide an initial insight to the necessary numerical modeling of the non-equilibrium conditions in PPTs. Presently, the thrust generation processes are only partially understood in spite of a continuous evolution of theories. Plasma ignition starts the complex sequence of events. An igniter is used to focus the electrical energy along the surface of the propellant. The solid surface is vaporized and the electrical circuit closes like a switch. The plasma particles are accelerated down the thrust chamber by the action of the applied magnetic field on the current. Experimental results demonstrate that the mass expelled is directly proportional to the energy discharged. The relatively low efficiencies of these thrusters has been a motivation to develop more accurate means of modeling the related phenomena.

The commonly used equations that define the operation of PPTs are as given below [16]. First we write the equations within the accelerator

Voltage: $$V = JR + \frac{d(LJ)}{dt} \qquad (5\text{-}4)$$

Power: $$P = JV = J^2R + J\frac{d(LJ)}{dt} \qquad (5\text{-}5)$$

Energy: $$W = \int P dt = \int \left(\underbrace{J^2R}_{OHMIC} + \underbrace{\tfrac{1}{2} J^2 \frac{dL}{dt}}_{INDUCTIVE} \right) dt \qquad (5\text{-}6)$$

Local Efficiency: $$h_e = \frac{\frac{1}{2}\int\left(J^2\frac{dL}{dt}\right)dt}{\frac{1}{2}CV_o^2} \quad (5\text{-}7)$$

Thrust: $$F = \frac{1}{2}J^2\left(\frac{dL}{dt}\right) = \frac{1}{2}J^2L' \quad (5\text{-}8)$$

LINEAR: $$F = \frac{1}{2}m_O(\frac{h}{w})J^2 \quad (5\text{-}8\ a)$$

COAXIAL: $$F = \left(\frac{1}{4p}\right)m_o \ln\left(\frac{r_o}{r_i}\right)J^2 \quad (5\text{-}8\ b)$$

Where L is the inductance, J the current, C the capacitance, R is the resistance, V_o is applied voltage, μ_o permeability of dielectric, h is the height between electrode and cathode, w is width of cathode and electrode, r_o is radius to outer electrode, r_i is radius to inner electrode.

Subsequently, the total performance equations for the mass bit ejected are as follows, where $\overline{u}_e$ is the exit mass-averaged velocity, $\dot{m}$ is the mass flow rate, g_o is the Earth's gravitational gradient:

Thrust: $$F = \dot{m}\overline{u}_e \quad (5\text{-}9)$$

Specific Impulse: $$I_{SP} = \frac{\overline{u}_e}{g_o} \quad (5\text{-}10)$$

Total Impulse: $$I_{bit} = \frac{1}{2}L'\int_0^t J^2 dt \quad (5\text{-}11)$$

Thrust to Power Ratio: $$\frac{F}{P} = \frac{I_{bit}}{\frac{1}{2}CV_o^2} \quad (5\text{-}12)$$

Efficiency: $$h_T = \frac{\frac{1}{2}m_{bit}\overline{u}_e^2}{\frac{1}{2}CV_o^2} = \frac{Kinetic\ \ Energy}{Capacitor\ \ Energy} \quad (5\text{-}13)$$

Optimizing the performance of PPTs, measured by impulse bit and specific impulse, is more than a linearly scaled problem. The different geometries and feed

variations introduce additional operational optimizing variations. Electrical arcs can be short-pulsed or quasi-steady: the duration of a short electrical pulse is less than the acoustic time in the thruster (the thrust chamber length/propellant velocity) so the thrust is generated from two discrete components. A longer electrical pulse enables quasi-steady flow which allows the gas dynamic propagation simultaneously with the electromagnetic thrust propagation. Thus, total thrust may actually be the result of two separate thrust effects: a gas dynamic (electrothermal) thrust and the above mentioned electromagnetic thrust. Since 1968 [16], experimental results have demonstrated that the gasdynamic pressure can contribute noticeably to the thrust component [16]. Because these two thrust modes optimize differently, it is important to establish the domain of each. In particular, Burton and Turchi [16] report that at the lower range of specific impulse, their co-axial, gas-fed device operates primarily in a gas dynamic mode.

The ablation surface area is one of the variables to control the ablated mass per joule. Typically a lower mass/energy ablation corresponds to a higher I_{sp} but a lower I_{bit}. Location and type of igniter used to initiate the plasma discharge is a way to produce pulse length variations in the discharge pulse. The igniter plug is a switched capacitor circuit that provides a high voltage, but low energy electric discharge.

The propellant can be altered, but Teflon® has superior I_{sp}, I_{bit}, and negligible surface char. Other fuels examined included: Kynar®, Viton®, Fluorel®, Kel-F®, Genetron®, Halon®, Delrin®, CTFE-2300®, Celcon®, Halar®, Tefzel®, polypropelene, and polyethylene. One of the more promising results was of a laminate bar with layers of Teflon® and polyethylene $[C_2H_4]_x$, (Figure 5-3). The fuel bar design is either rectangular or coaxial and side-fed or breech-fed. However, multiple fuel bars can be incorporated into a side fed design. The electrode plates are not restricted to parallel and straight cylinders. Using flared electrodes to create a high area ratio nozzle effect have improved the performance of some experimental thruster design. Furthermore, the nozzle can be ablating, non-ablating, or conductive. Each nozzle design has unique experimental results.

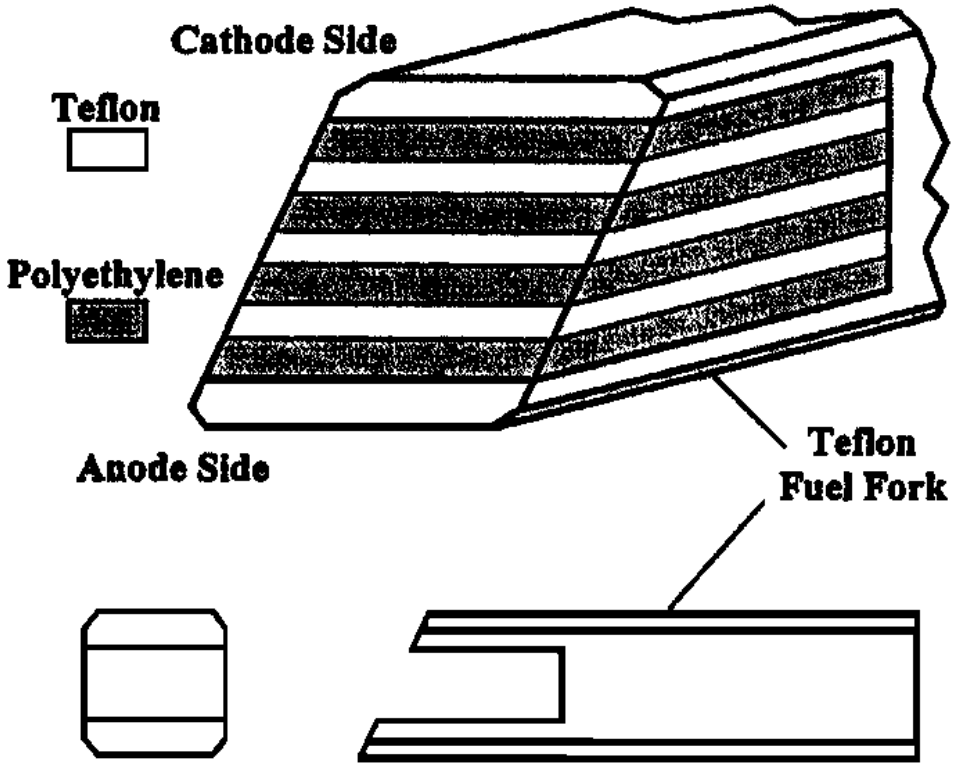

Figure 5-3. Optimizing Teflon Fuel design. [From 16]

Electrical discharge pulses generally oscillate in the form of a damped sine wave, as shown in Figure 5-4 and Figure 5-5. These oscillations create regions of reverse current and necessitate a trade off between lifetime and capacitor mass. Circuit designs have been determined to be critical to maximum thrust generation [16]. Figure 5-4 shows an early impulse waveform and Figure 5-5 depicts the refinements to design. Figure 5-6 is the corresponding electrical schematic of the University of Illinois's PPT-4 coaxial thruster. Figure 5-5 shows the improvements to the impulse wave and the schematic of a high impulse bit per joule thruster. The current pulse is non-reversing, due to the quenching diode (Figure 5-6), and the pulse length is short with respect to the acoustic properties of the thrust chamber. With these two factors, the electromagnetic thrust is generated prior to most of the gas dynamic thrust generation. The final PPT variation is through alterations to an applied magnetic field. An applied magnetic field, through permanent magnets or electro magnets, enhances the emf acceleration in a rectangular geometry.

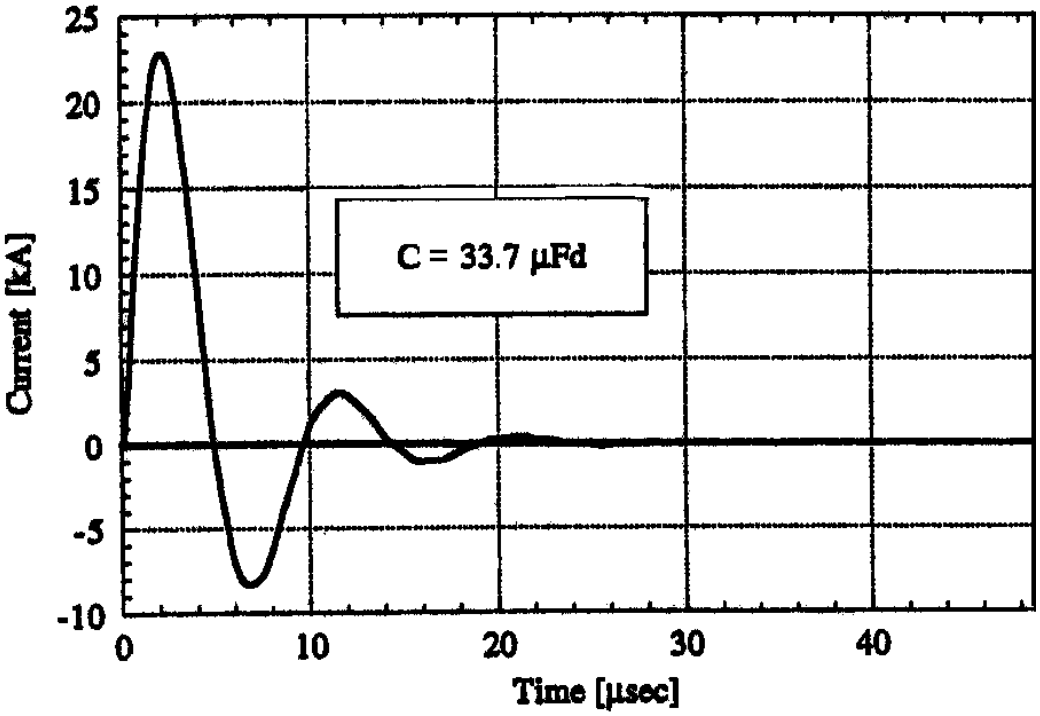

Figure 5-4. Current arc of Rectangular PPT Geometry. [From 16]

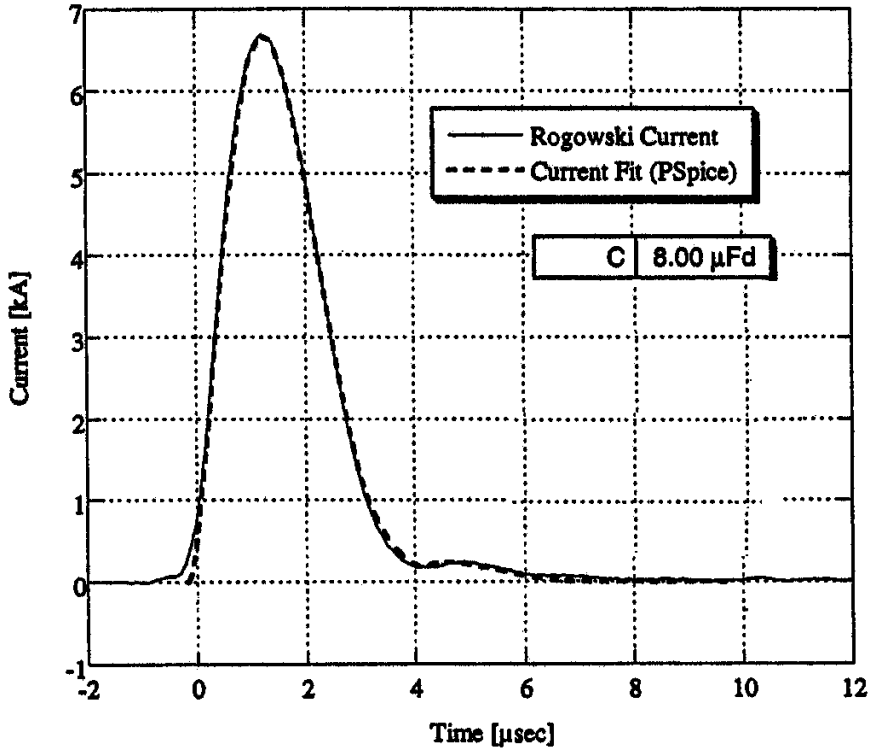

Figure 5-5. Current arc of Coaxial PPT with diode. [After 16]

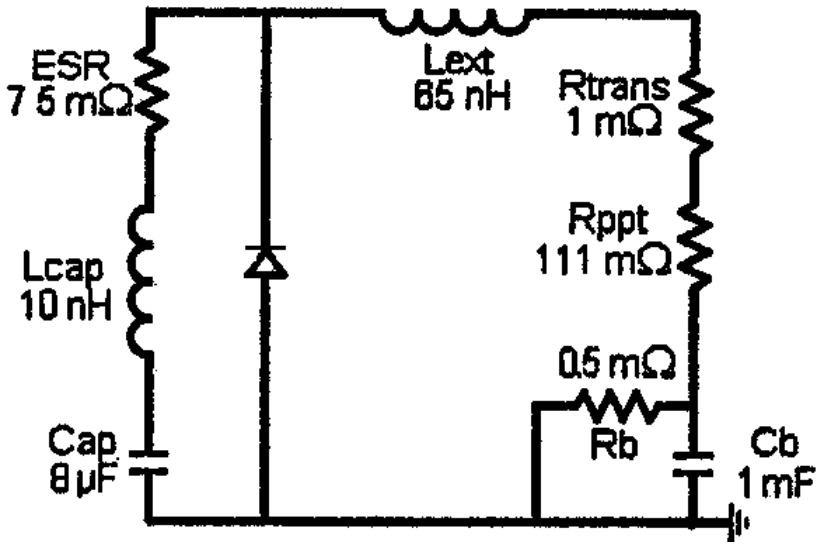

Figure 5-6. Schematic of PPT-4, notice quenching diode. [From 16]

The limited ability to perform numerical modeling limits design improvements to largely empirical methods. Many unresolved questions concerning PPTs will keep experimental laboratories employed for many years. Some of the present theoretical models include: describing the electrical discharge pulse as ultraviolet radiation from the igniter spark to free the electrons along the propellant surface and subsequently charge the macro particles [16]. Mass spectrometer studies of the exhaust plume provide information on exhaust mass propagation. This information is applied to the numerical programs like NASA's MACH2 or Los Alamos' SESAME. An interesting result is that 48% of the thrust is generated from gasdynamic forces and 52% from electrogmagnetic force [17]. This information enables other models to apply gas dynamic approximations to the quasi-steady thrust chamber. Most methods used allow for small design improvements, but are limited due to the complicated nature of the PPT device [17].

Figure 5-7 shows a breakdown of the energy losses and efficiencies encountered within the PPT. The efficiency abbreviations used are: power plant unit (η_{PPU}); capacitor and transmission line (η_{trans}); sheath (η_{sh}); heat loss through walls and evaporation (η_{heat}); total plasma ions and neutrals (η_F); thrust (η_t); overall system (η_o). Based on component estimates and frozen flow efficiencies the predicted maximum efficiencies (η_t) are 44% for rectangular PPTs and 60% for coaxial PPTs. [17]

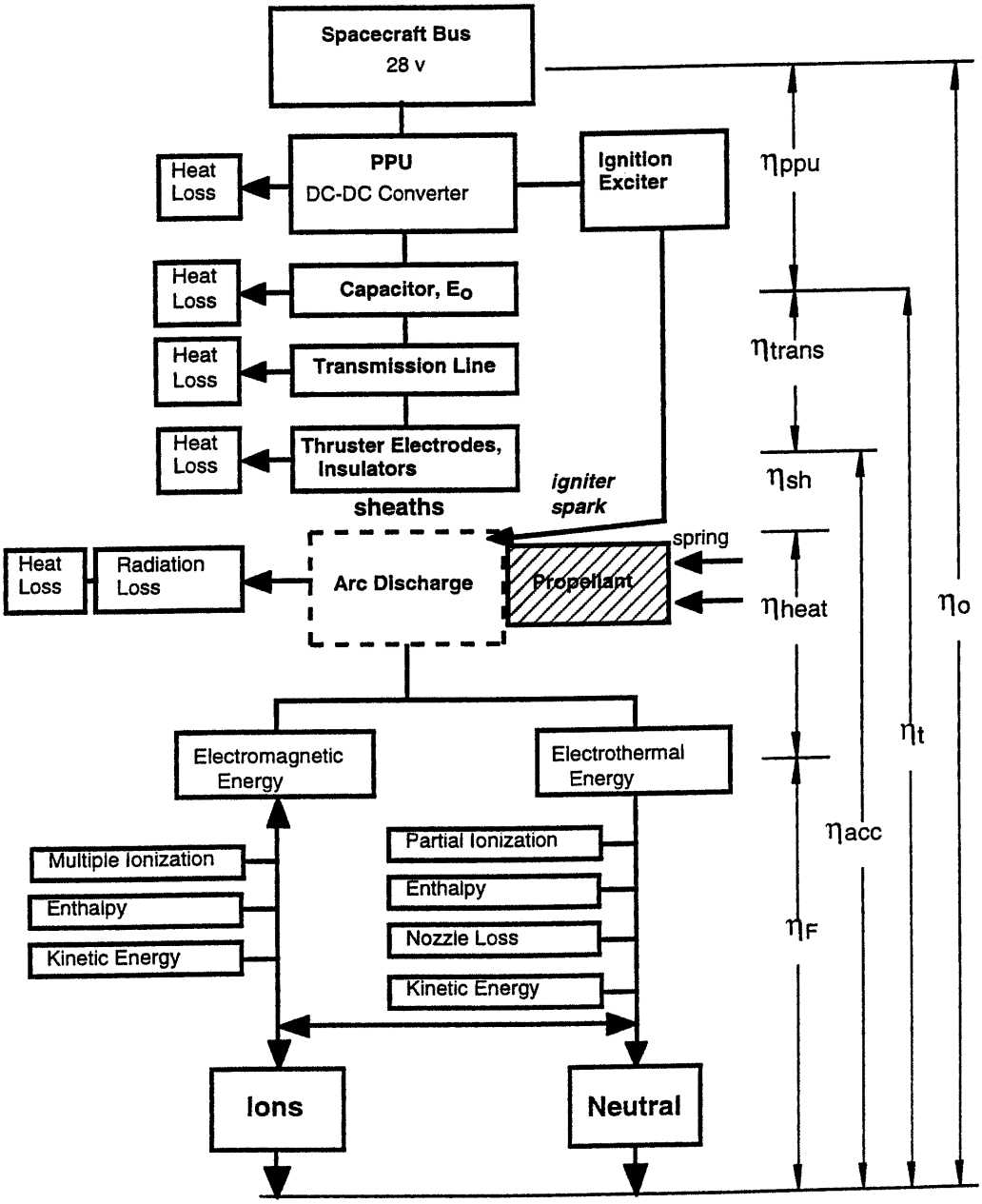

Figure 5-7. Breakdown of the Energy Processes and Efficiencies within the PPT. [From 17]

C. DISADVANTAGES

Electomagnetic Interference (EMI) is a primary consideration against the use of the PPT in spacecraft. EMI issues are resolved with good shielding techniques and certain PPT design options. The rectangular geometric form uses a current loop to generate the electromagnetic thrust. Unfortunately, this current loop acts also as an antenna. The initial discharge arc creates another short duration electromagnetic

radiation source antenna. Additionally, the charged plasma discharge introduces more electromagnetic emissions into the spacecraft's local environment. Measured frequency interference is in the 0.2-18 GHz range. External magnetic coils can be used to provide shielding, but this creates an additional mass. The large EMI of the electromagnetic thrust can be removed by switching to an axis-symmetric configuration. In which, the discharge pulse remains a shielding issue and the charged effluent is unavoidable. Fortunately, the total radiated power is in the milliwatt range and a good communication subsystem can compensate for such added background radiation. [17]

The exhaust effluent is significantly less than other propulsion systems, but the charged carbon ions pose a design problem. A good mission operations plan can resolve these design challenges. A spacecraft with an optical payload should choose an alternative propulsion system because charged macro particles are unavoidable when using a PPT propulsion system.

The earliest designs were bulky and difficult to space qualify because of the size and mass of the power conditioning equipment. Present efforts to increase efficiencies and reduce the thrust requirements are likely to ease these problems.

D. USAGE

PPTs are among the best candidates for miniaturization. The smaller discharge gaps and accelerating geometries may allow the use of the more compact ceramic capacitors [17] and perhaps towards the elimination of capacitors altogether. To meet the goal of reducing the thruster size and mass, the best candidate is a coaxial micro PPT. The electrical design is simpler and allows a reduced mass. Air Force Research Laboratory (AFRL) [18] has investigated the miniaturization process and produced a viable micro-PPT (Figure 5-8). This small thruster has been reduced in total mass of 80 g and tested for 10^6 firings with an average thrust of 50 μN. A launch date of 2003 on TECHSAT21 with additional usage on other Air Force satellite projects in the subsequent future will provide a flight heritage for this PPT. [19]

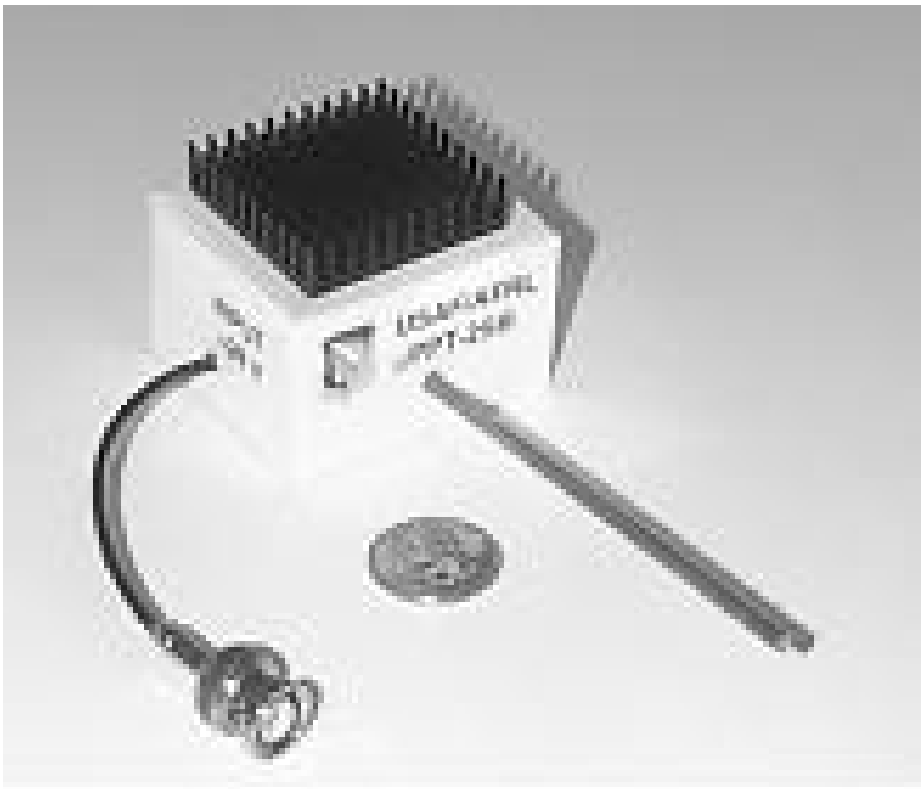

Figure 5-8. Air Force Research Lab's mPPT. [From 18]

VI. SPACE MISSIONS

A. MISSION PLANNING

There are design tools used to assist the spacecraft design team to determine an appropriate propulsion system. Table 4-1 and Figure 6-1 are two such tools. Figure 6-1 depicts the specific impulse different experimental microthrusters are able to provide and the subsequent electrical power requirements. Estimated power requirements for station keeping, attitude control, and orbital changes are based on estimated specific power (α) and estimated propulsion masses (m_{pp}) for a 1 kg spacecraft with a three year mission. Sutton and Biblarz [6] estimate the electrical power (P_e) in equation 6-1. Additional terms used are thruster efficiency (η_t), gravity gradient (g_o), mass flow rate ($\dot{m}$) and specific impulse (I_{sp}).

$$P_e = \alpha m_{pp} = \frac{1}{2\eta_t}\dot{m}\left(I_{sp}g_o\right)^2 \tag{6-1}$$

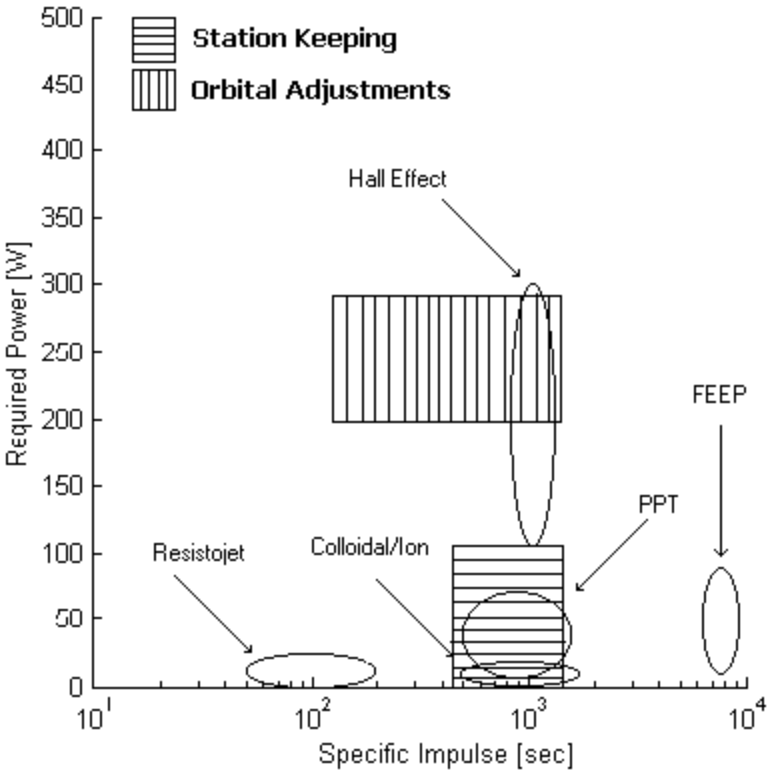

Figure 6-1. Overview of application regions for different electrical microthruster options.

As the satellite mission is lengthened, the propellant mass becomes a significant factor in determining an appropriate propulsion system. Figure 6-2 is a graphic from a cooperative effort between Jet Propulsion Laboratory and Primex corporation for a moderately active propulsion system. [20] With a short mission duration, there is little difference between propulsion options, but as shown a long mission makes the initial attractiveness of Cold Gas, Resistojet, or Hydrazine propellants fade.

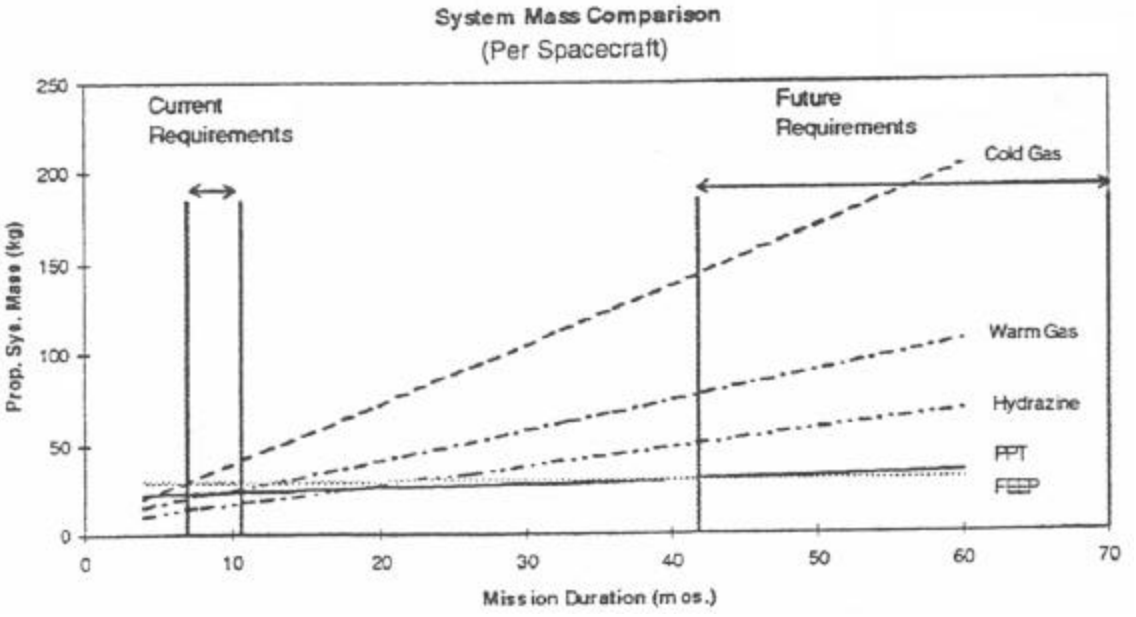

Figure 6-2. Mission Comparison of Propulsion System Masses modified from reference. [After 20]

B. SCHEDULED MISSIONS

The incorporation of a propulsion system to meet the mission requirements is critical to spacecraft design. Small satellites were the first to be designed and launched. Vanguard I was more than a simple radio transmitter in an elliptical earth orbit. Vanguard's small design reflected the 1950's launch system's technological limitations, yet it was a test platform for solar power, atmospheric mapping, and other astronautical experiments used in later spacecraft designs. After many years technological advances enable modern satellites larger than a Greyhound bus to be placed into any orbit. Multiple business ventures have once again generated a need for small satellites equipped with highly advanced payloads. The technology required for microsatellite design

requires proven performance. The following missions are designs that will prove the MEMS and microtechnologies capable of providing the necessary system designs.

1. Vanguard I (Launched March 17, 1958)

The first solar powered United States Satellite ever launched was a pico-satellite, shown on test stand in Figure 6-3. The fist U.S. satellite was Explorer I, launched January 31, 1958 on a Redstone rocket. [21] Vanguard I was initially designed as a simple nose cone in 1956 the decision was made to launch a small 1.47 kg satellite. This test satellite consisted of a simple 16 cm polished aluminum alloy sphere equipped with two transmitters operating at frequencies centered around 108 MHz. A satellite without a propulsion system is generally called a tumbler. Without the ability to correct for orbital decay a tumbler satellite generally has a limited orbital lifetime before the orbit decays and the satellite is destroyed upon reentry. Vanguard I was placed into an orbit that would require many years before it enters the lower atmosphere. It is currently the oldest artificial satellite. Vanguard I was placed into a highly elliptical orbit with the apogee altitude of 3866 km and perigee of 656 km and a period of 134 minutes. [22]

Figure 6-3. Vanguard I on Test Stand 1956. [From 22]

2. OPAL (Launched January 26, 2000)

Opal (Orbiting Picosatellite Automated Launcher) is a Stanford University built satellite (shown in Figure 6-4) and was launched aboard an Air Force rocket on January 26, 2000. As the first satellite in the University Satellite Program, its successful primary

mission was to demonstrate the feasibility of launching multiple picosatellites from a mothership satellite. The satellite's secondary payloads are an accelerometer test bed and a magnetometer test bed used to perform component characterization. Two of OPAL's three payloads test the behavior of MEMS devices in space. These payloads are the accelerometer and the picosatellite payload to investigate new mission architectures that will require the application of MEMS technologies in the future. [23]

Figure 6-4. OPAL in pre-launch testing. [From 23]

The primary mission of the OPAL picosatellite payload was to provide an end-to-end mission demonstration of mothership and daughtership technologies. The OPAL mothership stored and deployed six picosatellite daughterships without propulsion (three are shown in Figure 6-5), although the DARPA/Aerospace pico satellites were tethered together. These daughter satellites were designed and constructed by a team from DARPA, the Aerospace Corporation, Santa Clara University, an amateur radio (HAM) team. [23]

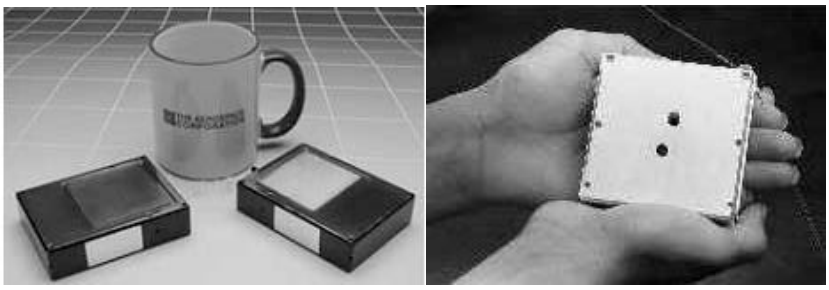

Figure 6-5. Aerospace Corporation's Daughter Satellites (left) and Santa Clara's Artemis Satellite (right).[From 23 and 24]

3. Snap-1 (Launched June 28, 2000)

On June 28, 2000, two European companies, the Surrey Satellite Technology Limited (SSTL) and Polyflex Aerospace, as part of the University of Surrey's Surrey NanoSat Applications Programme (SNAP), placed the smallest functioning propulsive satellite into orbit. SNAP-1 is a 6.5 kg, 3-axis stabilized, imaging satellite. The propulsion system is a single cold-gas thruster with a subsystem mass of 450 g with 32.6 g of liquid fuel. Figure 6-6 depicts the schematic of the SNAP-1 propulsion system. Butane (C_4H_{10}) is the liquid gas fuel which provides an I_{sp} of 70 sec through the Polyflex thruster (throat area (A_t) of 420 nm, area ratio (A_3/A_t) of 208:1) at a chamber pressure (p_1) of 2.1 bar and chamber temperature (T_1) of 20° C. The liquid gas is easier to store and easily heated beyond its vapor pressure and released through the thruster as a cold gas. [25]

The first satellite of a small satellite series, SNAP-1 operates in the amateur radio band, is largely compatible with previous amateur radio satellites in the UoSAT-OSCAR satellite series. The mission purpose of SNAP-1 was to demonstrate the feasibility of a standardized modular nanosatellite bus, to provide a test-bed for novel microelectronic technologies - in particular a new GPS navigation system, APD camera technologies and RISC processors, provide experimental and imaging data to the radio-amateur/amateur-scientific communities, and to provide a vehicle for the education and training of students in spacecraft engineering at an undergraduate and graduate level. The mission has been successful in all areas. [26]

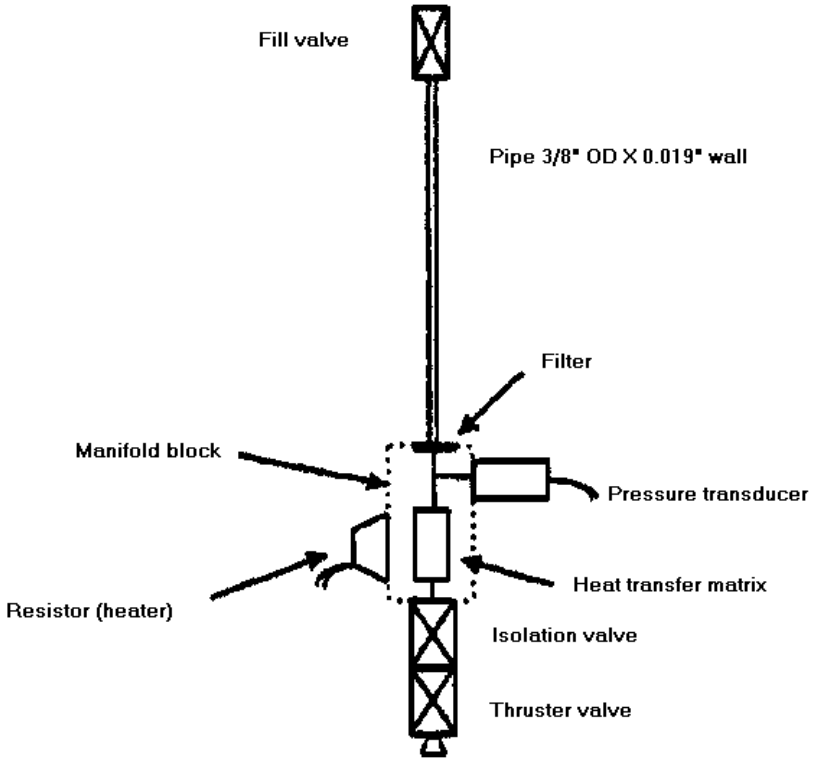

Figure 6-6. SNAP-1 propulsion subsystem. [From 25]

4. University Nanosatellite Program

The Air Force Office of Scientific Research (AFOSR) and the Defense Advanced Research Projects Agency (DARPA) have jointly funded 10 university research projects for the design and demonstration of university built nanosatellites (1-10 kg). The goal is to demonstrate miniature bus technologies, formation flying, and distributed satellite capabilities. The satellites have planned launch dates during 2003. [27]

The Air Force Research Laboratory (AFRL) is designing the deployment structure for these 10 nanosatellites, securing a launch, and providing microsatellite hardware such as high efficiency solar cells and micropropulsion units. NASA Goddard has also joined the program and is currently providing $1.5M funding to demonstrate crosslink communications, navigation hardware, and flight control algorithms to assist with formation flying. [28]

The universities selected for the program (and their missions) are: Arizona State University, University of Colorado at Boulder, and New Mexico State University (Three

Corner Sat); Stanford University and Santa Clara University (Emerald); Stanford and MIT (Orion), Utah State University (USUSat); Virginia Polytechnic Institute and State University (Hokiesat); University of Washington (Dawgstar). The ten universities are broken down into two flight missions: Nanosat-1 and Nanosat-2. Nanosat-1 is the first mission consisting of Emerald (Stanford University and Santa Clara) and Orion (MIT and Stanford University). Nanosat-2 is the second mission is made up of ION-F (Utah State University, University of Washington, and Virginia Tech) and Three Corner Sat (Arizona State University, University of Colorado at Boulder, and New Mexico State University). [27]

a. ***Nanosat-1 (Expected Launch date: April 2003)***

Nanosat-1 is scheduled to launch on board the Space Shuttle in April of 2003. This will include Emerald and Orion satellites.

Emerald is the pre-cursor to AFRL's TechSat 21 University Nanosatellite Program. The Techsat 21 program is an investigation into the use of microsatellite clusters to perform space missions for the 21st century. Stanford University and Santa Clara University are developing EMERALD, as a low cost, two-satellite mission to validate formation-flying technologies. Emerald's mission is to transform from a single satellite to two free flying satellites in a coarse formation to permit simple demonstrations of fundamental formation flying control functions such as relative position determination and position control. [27]

Emerald will also demonstrate a technology for future MEMS propulsion systems, the advanced colloid microthrusters. These microthrusters will enable small-scale position control and can supply vectored thrust on the order of 0.11 mN with an I_{sp} of 100 sec. These components are currently in development by Stanford's Plasma Dynamics Laboratory. [11]

b. ***Nanosat-2 (Expected Launch date: June 2003)***

Nanosat-2 is scheduled to launch on board the Space Shuttle in June of 2003. This will include Three Corner Sat (3CS) and ION-F satellite programs.

(1). Three Corner Sat Constellation (3 C S)

This satellite constellation is produced as the cooperative efforts of three universities: Arizona State University (ASU), University of Colorado at Boulder (CU), and New Mexico State University (NMSU). Figure 6-7 shows the intended launch configuration and location of each satellite. Each university has a focus area for development and design and each university will build a satellite based on the cooperatve designs. The mission of this three satellite constellation is to demonstrate stereo imaging, formation flying/cellular phone communications, and innovative command and data handling. The three satellites will fly in a linear follow-formation with relatively constant separation from each other. Stabilization for the satellites is gravity gradient with +/- 5 degrees pointing accuracy. Each satellite has a Satellite Processor Board to serve as the local controller, data interface, on-board memory, and processor. The Satellite Processor will be responsible for supervising the operation resource management of the satellites. [28]

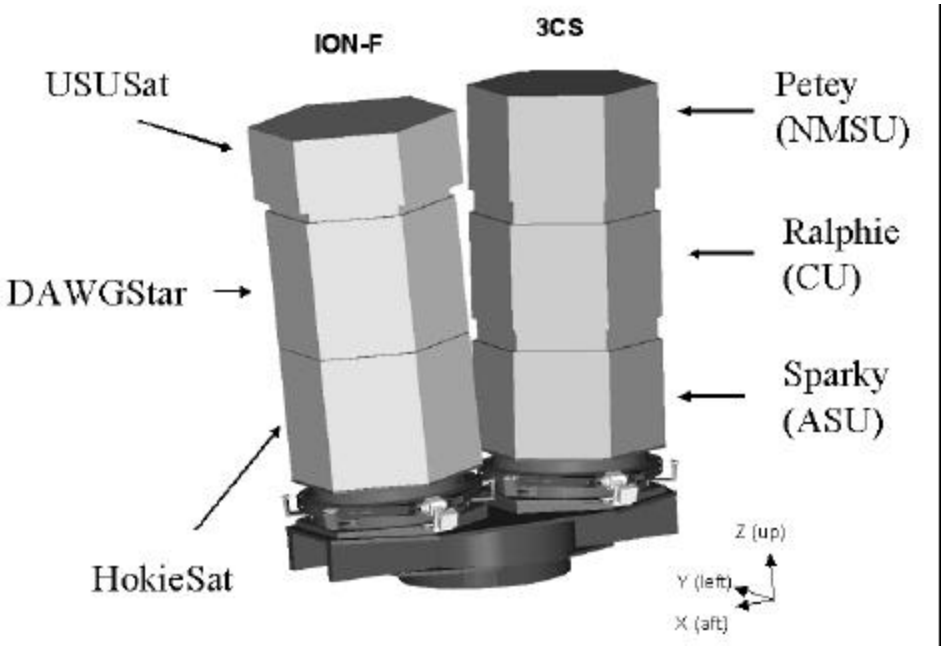

Figure 6-7. Possible Launch Configuration for Three Corner Sat and ION-F. [After 28]

The Free Molecular Micro-Resistojet (FMMR), initial plans incorporated it into the 3CS design as an experimental propulsion system, will not be an active element of the satellite propulsion system. Due to time and funding, only a heater chip (Figure 6-8) will be flown for testing. Four of these devices will be on each satellite (Petey, Raphie, and Sparky). This experiment will test the chip survivability from launch to the space environment and provide information on propulsion capabilities of this device. The operational characteristics such as power consumption and the thermal profile will also be measured. The FMMR is 13 mm wide and 42 mm long and is 0.4 mm thick. The total weight of this device including the Teflon® housing unit is under 0.5 kg and the heater strip consumes 3 W. [28]

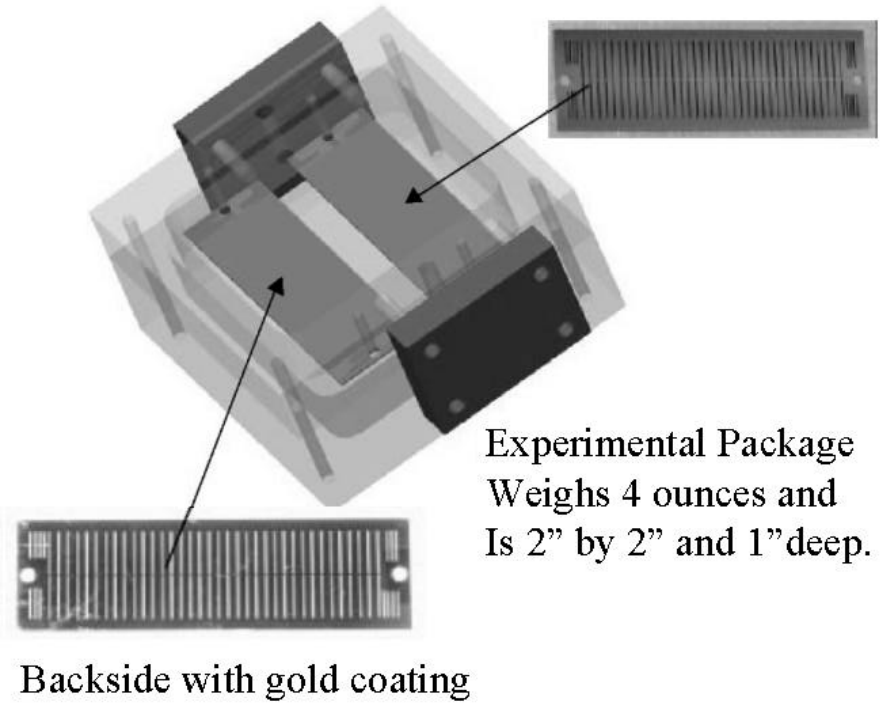

Figure 6-8. Free Molecular Micro-Resistojet heater strip developed by Arizona State University for each 3CS. [From 28]

(2). ION-F

Utah State University, University of Washington, and Virginia Polytechnic Institute are designing and developing a system of three 10 kg spacecraft to investigate satellite coordination and management technologies and distributed ionospheric measurements. The three satellites consisting of USUsat, Dawgstar and Hokiesat, respectively, will coordinate on satellite design, formation flying and management mission development, and science instruments and mission. A rectangular micro Pulsed Plasma Thruster, as shown in Figure 6-9, is the primary attitude control propulsion for each satellite that utilizes a propulsion subsystem. This PPT weighs approximately 0.5 kg. Adding the electrical power conditioning unit and eight thruster increases the propulsion system mass to 4 kg for each satellite. Additionally, an internet based operations center will enable each university to control its satellite from an on campus remote location. ION-F will focus on mission objectives to benefit TechSat 21 and future missions of the Air Force and NASA. Formation flying will be accomplished by the use of a cross-link communication system developed at Johns Hopkins Applied Physics Laboratory. [29]

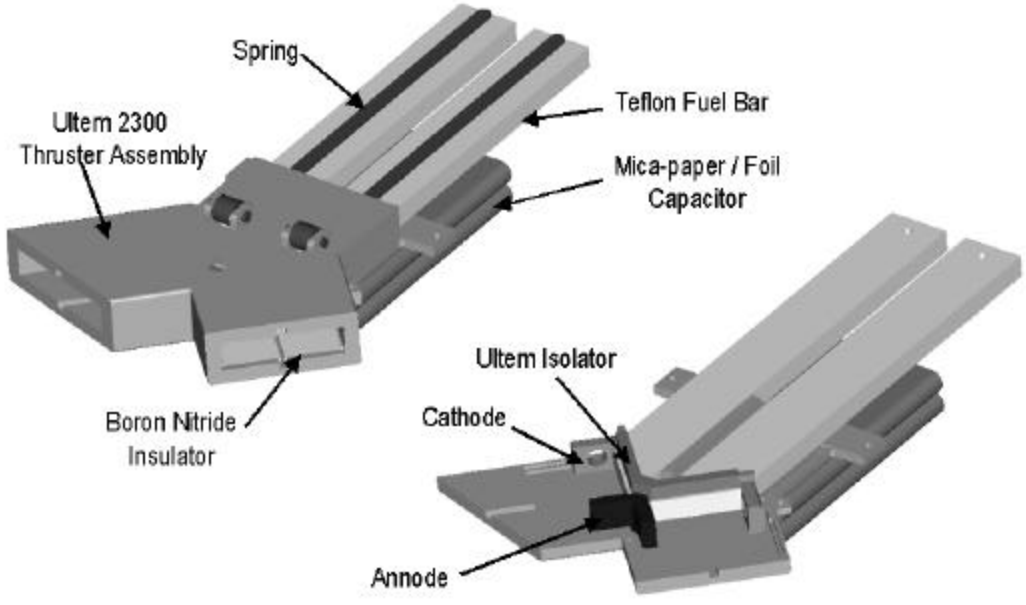

Figure 6-9. ION- F Micro Pulsed Plasma Thrusters. [From 29]

5. TechSat 21

TechSat 21 is AFRL's investigation into the use of microsatellite clusters to perform space missions. Planned research on sparse aperture sensing, ionospheric effects, and MEMS technology for spacecraft. An overview of the TechSat 21 design is shown in Figure 6-10. The design will address the problem of Ground Moving Target Indication (GMTI), in which slow moving targets are detected against large ground clutter. [19]

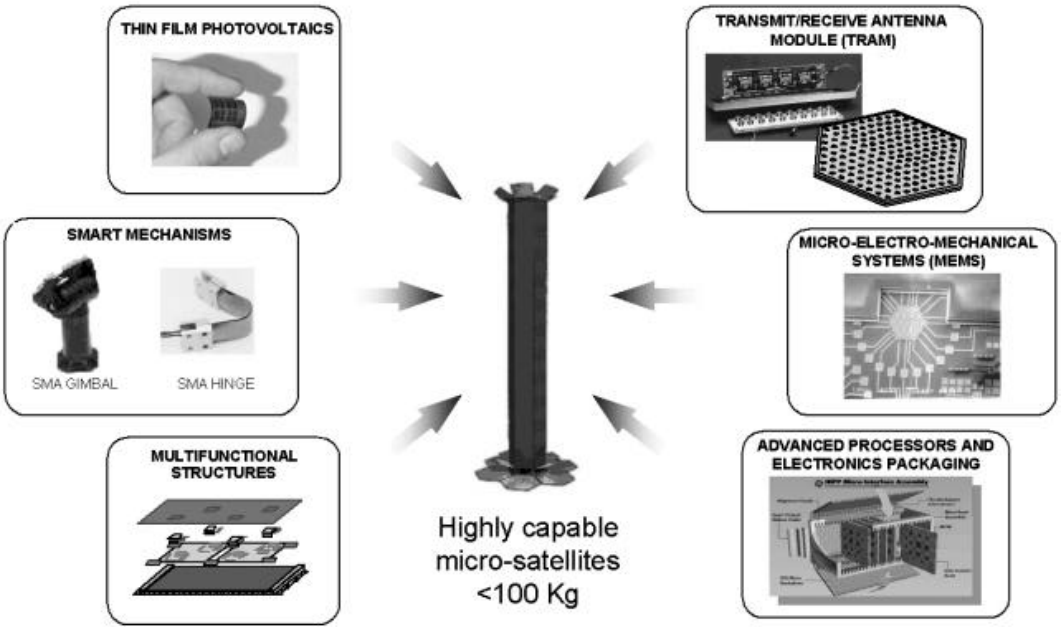

Figure 6-10. TechSat 21 Mission Concept. [From 19]

The design consists of each satellite transmitting a signal orthogonal to the others, while receiving and coherently detecting the returned signal from other satellites' transmission, including its own. Since the coherent response at each satellite is individually sampled, the array provides angle-of-arrival information about the scattering from a given target in both the azimuth and elevation directions. This constellation of satellites is anticipated to be roughly 100 meters in extent, and would consist of approximately 4 to 20 satellites. [19] An important advantage of the distributed aperture system over a monolithic system is the ability to dynamically reconfigure to perform multiple missions. One example of a multi-mission role is the ability to perform the radar

mission simultaneous with a geolocation application. Extending the satellite's baselines can also increase accuracy in geolocation missions. [19]

The main propulsion system of each satellite is MIT's 50 W Hall Thruster. This propulsion system is strictly for orbital adjustments. The AFRL micro-PPT will be included as an experimental thruster system to be tested in space and provide proven performance. [30]

VII. CONCLUSION

A. PRESENT WORK

Extensive experimental research work has led to the very capable microthrusters discussed. In the near future these micropropulsion systems will be incorporated into spacecraft and their subsequent success or failure will determine which thruster arrangements will survive into the next generation of small satellite design. To meet propulsion requirements for one kilogram picosatellites or ten kilogram microsatellites, reliable and efficient microthrusters will meet the low thrust requirements. Many independent researchers have contributed greatly to areas of micropropulsion, but as yet, no one has started to integrate the various findings into similar packages. The best example of concurrent research efforts is the work done at MIT by Bayt [10] and the work at Aerospace Corp by Janson [8]. Bayt developed a refined 2D MEMS nozzle and Janson developed an integrated MEMS fluid transport system yet, insisted on using under-optimized nozzles. A collaboration of their efforts would provide an excellent propulsion system for one kilogram satellites.

B. CANDIDATES

Through the presentation of different micropropulsion technologies, the question of using MEMS to replace conventional components has been addressed. Through the incorporation of MEMS sensors into large propulsion systems the spacecraft mass can be reduced. Additionally, a micropropulsion system can replace entire secondary propulsion systems and reduce the spacecraft mass. There is an endpoint beyond which the usefulness of an integrated MEMS propulsion system becomes irrelevant and the mission design would be better to include a spacecraft without any propulsion system. The boundary layer problem demonstrates size limitations of coldgas and warmgas microthrusters. However, electrical pulsed plasma thrusters and laser ablation microthrusters do not use a DeLaval nozzle and can achieve even smaller thruster dimensions. The problem associated with any reduction in scale of a plasma thruster is containment of the electric field. However, the added advantage of reducing the size of a pulsed plasma thruster is the lower power requirements. Eventually the storage capacitor could be removed and the ablation arc can be powered from a small mass power-

conditioning unit. The end result will revolve around the mission cost. MEMS can significantly reduce the cost of fabrication and launch with little effect on design costs. Where and how to integrate MEMS into spacecraft design remains up to the designers. MEMS can play a key role and with proven flight heritage and reliability more system engineers will integrate MEMS into their designs.

The goal of some MEMS researchers is to achieve an integrated spacecraft less than one millimeter in diameter. Unfortunately, some futurists have predicted that these independent microsatellites will be integrated onto one large microsurface orbiting the Earth. Satellites of this nature and size will lack the necessary de-orbit propulsion system to prevent an accumulation of space debris in terrestrial orbits. These integrated femptosatellites have a niche within the earth's atmosphere, as advanced sensor and communication arrays, but in space they will add to the clutter and any unique utility becomes highly questionable.

Wide arrays of microsatellite formations are able to provide a valuable service to terrestrial needs in space. Low cost does not have to also mean low reliability. There are many robust propulsion systems ready for the challenges of space travel. The Air Force Research Laboratory's micro Pulsed Plasma Thruster has achieved the first steps toward miniaturization: low mass, low power, and high reliability. The other pulsed propulsion systems that are only now emerging: laser ablation and vacuum arc ablation thrusters are similar candidates for future missions. The resitojet microthruster could be the means to provide an excellent main propulsion system for microspacecraft. Although the cost driven goal is to provide increasingly smaller satellites, large satellites and manned spacecraft will require other propulsion methods with large scale size restrictions. MEMS will be a crucial part of these larger thrust propulsion systems. Mass and power reduction will come through the use of MEMS devices as sensors and flow regulators. This technology is available today and requires proven flight heritage before the low cost will make their use widespread throughout the aerospace industry.

LIST OF REFERENCES

1. Public Broadcasting Service, "Miracle Month", Available: [http://www.pbs.org/transistor/background1/events/miraclemo.html], 1999.
2. Helvajian, Henry (editor), Microengineering Aerospace Systems, The Aerospace Company, El Segundo, La. 1999.
3. Thompson, V., "New Microsystems Applications Drive Fast Growth". Available: [http://www.smalltimes.com/document_display.cfm?document_id=3424], 2002.
4. Vallado, David A., Fundamentals of Astrodynamics and Applications, The McGraw-Hill Companies, Inc., New York, NY. 1997
5. Sidi, Marcel J., Spacecraft Dynamics & Control: a practical engineering approach, Cambridge University Press, New York, NT. 1997.
6. Sutton, George P. and Biblarz, Oscar, Rocket Propulsion Elements: An Introduction to the Engineering of Rockets, 7th Ed, John Wiley and Sons, Inc, New York, NY. 2000.
7. Beatty, Thomas, "Rocketry", Available: [http://lifesci3.arc.nasa.gov/SpaceSettlement/teacher/lessons/contributed/thomas/rocket/rocket.html#INTRO], 1999.
8. Janson, Siegfried W, Huang, Adam, Hansen, William W., Helvajian, Henry, "A microengineered cold gas thruster system for a Co-Orbiting Satellite Assistant (COSA)", The Aerospace Company, El Segundo, CA.1999.
9. Zakirov, V., Gibon, D., Sweeting, M., Reinicke, B., Bzibziak, R., Lawrence, T., "Specifics of Small Satellite Propulsion: Part 2", AIAA Paper 2001-3834, 37th AIAA Joint Propulsion Conference, Salt Lake City, Utah, 8-11 July 2001.
10. Bayt, Robert L., Analysis, Fabrication and Testing of a MEMS-based Micropropulsion System, Ph.D. Thesis, MIT, FDRL TR 99-1, 1999.
11. Micci, Michael M., Ketsdever, Andrew D. (Editors), Micropropulsion for Small Spacecraft, Progress in Astronautics and Aeronautics, Vol. 187, American Institute of Aeronautics and Astronautics, Inc., Reston, VA. 2000.

12. Lewis, David H., Janson, Siegfried W., Cohen, Ronald B., Antonsson, Erik K., "Digital MicroPropulsion", Sensors and Actuators A, Physical, Vol. 80, 2000.

13. Bayt, Robert L. and Breuer, Kenneth S., "A Silicon Heat Exchanger with Integrated Intrinsic-Point Heater Demonstrated in a Micropropulson Application", Sensors and Actuators A, Vol. 91, 2001.

14. Mueller, Juergen, Chakraborty, Indrani, Bame, David, Tang, William, Lawton, Russel, Wallace, Andrew, "Proof-of-Concept Demonstration of a Vaporizing Liquid Micro-Thruster", AIAA Paper 1998-3924, 1998.

15. Ziemer, John K., "Laser Ablation Microthruster Technology", AIAA Paper 2002-2153, 33rd AIAA Plasmadynamics and Lasers Conference, Maui, HI, 20-23 May 2002.

16. Burton, R. L. and Turchi, P. J., "Pulsed Plasma Thruster", Journal of Propulsion and Power, Vol. 14, No.5, September-October 1998.

17. Burton, Rodney L., Wilson, Michael J., Bushman, Stewart S., "Energy Balance and Efficiency of the Pulsed Plasma Thruster", AIAA Paper 98-3808, 34th AIAA Joint Propulsion Conference and Exhibit, Cleveland, OH, 12-15 July, 1998.

18. "New Satellite Propulsion System Has Mass Below 100 grams", AFRL Technology Horizons, Vol. 2, No. 4, December 2001.

19. Cobb, Richard "TechSat 21: Developing Low-Cost, Highly Functional Micro-Satellite Clusters for the 21st Century Air Force Missions", AFRL, 1999.

20. Cassady, R. J., Willey, M. J., Mechel, N. J., Blandino, J. J., "Pulsed Plasma Thruster for the New Millennium Space Interferometer Experiment DS-3", AIAA Paper 1998-3326, 34th AIAA Joint Propulsion Conference and Exhibit, Cleveland, OH, 13-15 July, 1998.

21. Lethbridge, Cliff, "Spaceline - Covering the Past, Present and Future of Cape Canaveral – Explorer I", Available: [http://www.spaceline.org/explorerchron.html], 2000.

22. Edstrom, Tommy, Vanguard website (keywords Vanguard satellite Sweden), Available: [http://home5.swipnet.se/~w-52936/index20.html], 2002.

23. Stanford Official OPAL Homepage, Available: [http://ssdl.stanford.edu/aa/projects/squirt2/index.html], 2002.

24. Okano, Elizabeth S., Microelectromechanical Systems for Small Satellite Application, Thesis, Naval Postgraduate School, Monterey, CA, June 2001.

25. Gibbon, D., Paul, M., Smith, P., M[c]Lellan, R., "The use of Liquified gasses in Small Satellite Propulsion Systems", AIAA Paper 2001-3246, 37th AIAA Joint Propulsion Conference Salt Lake City, UT, 8-11 July, 2001.

26. Surrey Satellite Technology website, Available: [http://www.sstl.co.uk/missions/subpage_missions.html], 2002.

27. Martin, Maurice, Schlossberg, Howard, Mitola, Joe, Weidow, Dave, Peffer, Andrew, Blomquist, Richard, Campbell, Mark, Hall, Christopher, Hansen, Elaine, Horan, Stephen, Kitts, Chris, Redd, Frank, Reed, Helen, Spence, Harlan, Twiggs, Bob, *University Nanosatellite Program* IAF Symposium, Redondo Beach, CA. April 1999.

28. Motola, Michael and Egan, Lauren, "University Nanosatellite Program: Three Corner Sat (3Csat)", Washington DC Presentation, January 31, 2001.

29. Rayburn, C., Campbell, M., Hoskins W. A., Cassady, R. J., "Development of a Micropulsed Plasma Thruster for the Dawgstar Nanosatellite", AIAA Paper 2000-3256, 2000.

30. Bromaghim, D. R., Spanjers, G. G., Johnson, L. K., Gorecki, R., Tan, F. D., Vondra, R., Pote, B., Barbarits, J., "The AFRL TechSat 21 Propulsion Subsystem Development Program", IEPC Paper 2001-165, International Electric Propulsion Conference 16 Oct 2001.

THIS PAGE INTENTIONALLY LEFT BLANK

INITIAL DISTRIBUTION LIST

1. Defense Technical Information Center
   Ft. Belvoir, Virginia

2. Dudley Knox Library
   Naval Postgraduate School
   Monterey, California

3. George P. Sutton
   11939 Gorham Avenue
   #302
   Los Angeles, CA 90049-5363

4. Brij Agrawal
   Naval Postgraduate School
   Monterey, California

5. Oscar Biblarz
   Naval Postgraduate School
   Monterey, California

6. Max Platzer
   Naval Postgraduate School
   Monterey, California

7. Jose Sinibaldi
   Naval Postgraduate School
   Monterey, California

8. Scott Lemay
   Naval Postgraduate School
   Monterey, California